UNIVERSITY OF ZIELONA GÓRA

CIVIL AND ENVIRONMENTAL ENGINEERING REPORTS

E-ISSN 2450-8594

CEER 2025; 35 (3): 0221-0254
DOI: 10.59440/ceer/207954
Original Research Article

DESIGNING FOR FLOW: HOW BAFFLE GEOMETRY SHAPES WOOD ACCUMULATION IN FISHWAYS

Jan BŁOTNICKI[1]
Wrocław University of Environmental and Life Sciences, Institute of Environmental Engineering, Wrocław, Poland

Abstract

The transport and accumulation of woody debris in watercourses play a significant role in shaping river morphology and supporting ecosystem functioning. However, these processes can also pose a threat to hydraulic infrastructure. Accumulation is particularly problematic in fish passes, where it reduces hydraulic capacity and impedes the migration of aquatic organisms. This study experimentally investigated how the shape of fish pass baffles influences debris retention and how log length affects blockage susceptibility. Two configurations were tested: one with rectangular baffles and another with rounded ones. The results showed that log length had a statistically significant effect on the accumulation rate (Effective Accumulation, EA), with larger logs more likely to be retained in both configurations. The highest EA was observed for large logs in the rectangular variant (EA = 0.51), followed by the rounded variant (EA = 0.33). Small logs exhibited minimal accumulation (EA ≈ 0.04–0.05), and no significant differences between shapes were found in this class. Although the total EA was higher for the rectangular configuration (EA = 0.24) than for the rounded one (EA = 0.16), this difference was not statistically significant, highlighting the need for more detailed spatial and size-based analyses. The jamming effect was also observed, where newly introduced logs accumulated on previously retained ones, reinforcing the blockage over time. These findings suggest that both baffle geometry and log size are critical factors influencing debris retention in fish passes and should be carefully considered in their design to balance ecological and hydraulic functions.

Keywords: floating debris, driftwood, pier modification, environmental risk management, infrastructure protection

[1] Corresponding author: Wrocław University of Environmental and Life Sciences, Institute of Environmental Engineering, Grunwaldzki Sq. 24, 50-363 Wrocław, Poland, jan.blotnicki@upwr.edu.pl

1. INTRODUCTION

1.1. Fish pass functionality and debris problems

The transport of woody debris in rivers is a natural phenomenon [1] that plays a key role in riverine ecosystems [2], influencing the structure and dynamics of river channels [3,4]. Wood transported by the current encounters various hydraulic obstacles such as bridges, weirs, and fish passes, which can lead to local changes in hydraulic conditions and pose potential risks to the structural soundness of these installations [5–7]. Fish passes are hydraulic structures designed to restore the longitudinal connectivity of rivers, enabling the upstream and downstream movement of aquatic organisms past migration barriers [8]. Their proper functioning is essential for maintaining fish populations and biodiversity [9,10]. In the case of fish passes, the presence of woody debris can particularly disturb their functionality and limit the free migration of fish [11–13]. In bridge engineering, one of the structural strategies to reduce the negative impact of drifting wood is the application of appropriately profiled bridge piers [14], sometimes additionally equipped with deflectors [15]. A better understanding of the origin, composition, and ecological role of floating debris—especially wood—is therefore necessary to assess both the challenges and potential benefits it poses for riverine systems.

1.2. Characteristics and Role of Floating Debris

Various aspects of floating debris have been extensively addressed in the literature [16,17]. The term *floating debris* refers to all materials drifting on the surface of water bodies, including both natural and anthropogenic elements such as wood, vegetation, plastic waste, and ice fragments [18]. A substantial proportion of natural floating debris consists of wood—commonly referred to as *woody debris*—which plays a significant role in hydromorphological processes and the functioning of riverine ecosystems [19].

Woody debris enters rivers through processes such as bank erosion, tree mortality, windthrow, beaver activity, landslides, wildfires, or floods [20,21]. Once mobilized, it influences flow hydraulics and sediment transport, contributing to local erosion and deposition [22,23]. Numerous studies have demonstrated that wood in rivers stabilizes bed sediments, creates flow variability, and enhances habitat diversity [21,24,25].

Large pieces of wood, typically referred to as *Large Woody Debris* (LWD), are particularly important in shaping in-stream structures. By forming natural obstructions and zones of reduced velocity, LWD contributes to the creation of suitable habitats for fish and other aquatic organisms [21,22,24]. However, when wood accumulates near hydraulic infrastructure, it can also pose risks, including localized flow blockages and increased flood hazard—effects that have been documented near bridge piers and culverts [23,26,27]. In such cases, wood accumulation may initiate local scour or structural destabilization [26,28,29]. The process often begins when a large element becomes lodged, creating a nucleus around which smaller debris and sediments accumulate, forming stable blockages [29–31]. These processes have been observed in rivers worldwide and can lead to significant morphological and hydraulic changes.

In July 2020, a similar mechanism was observed on the Odra River within the Wrocław Water Node, where a large log became lodged near the bank, initiating the accumulation of additional elements—smaller wood fragments, sediments, and plastic waste [32–34] – ultimately forming a flow obstruction [16,35].

Wood accumulation processes are often initiated by the wedging of a large element, around which smaller fragments and sediments accumulate, leading to the formation of stable structures [29,36,37].

These interactions between woody debris and hydraulic structures illustrate the dual role of wood in river systems—as both a driver of habitat complexity and a potential hazard to infrastructure [22,25,38].

Despite its risks, woody debris is increasingly recognized as a functional element in river management. In ecological restoration projects, wood is deliberately reintroduced into rivers to recreate habitat complexity and support fish populations, particularly for salmonid species [21,24,39,40]. This highlights the need to consider wood not only as a hazard to be removed but also as a resource to be integrated into river corridor design and maintenance strategies.

1.3. Research motivation, objective and scope

This study investigates how the geometry of baffles in a vertical slot fish pass affects the accumulation of floating woody debris within its chambers. The experimental work was conducted in a hydraulic flume using a physical model consisting of four cross-walls, each composed of five baffles spanning the channel width. Two structural variants were tested: the original configuration with rectangular baffles (K0) and a modified version with rounded baffles (K1).

The motivation for undertaking this research stemmed from long-term observations of debris accumulation at the fish pass adjacent to the Opatowice Weir on the Odra River (Poland), where this issue has been systematically monitored since 2018 [41]. While the laboratory model was not a full-scale replica of this facility, its geometric configuration—including the spacing between cross-walls, baffle arrangement, bed slope, and hydraulic conditions—was based on the design and operating parameters of the Opatowice fish pass, which served as a reference structure**.**

Previous research [41] indicated that rounded baffle[2] shapes may offer hydraulic advantages for fish passage compared to rectangular forms. Building on these findings, this study experimentally investigates how such structural features influence the accumulation of woody debris within fish pass chambers. Specifically, the study aimed to:

(1) compare the Effective Accumulation (EA) of wood for two baffle shapes forming the cross-wall configuration of a fish pass model,

(2) assess the influence of log size on accumulation dynamics, and

(3) evaluate how accumulation varies with the position of the cross-wall along the flow path, i.e. at the upstream (cross-wall 1), middle (cross-wall 2), and downstream (cross-wall 3) sections of the fish pass.

This is the first publication addressing the issue of woody debris accumulation within fish passes. To date, researchers worldwide have not focused on reducing debris accumulation inside fish passes by modifying structural elements [41]. Rather than addressing internal structural modifications, earlier studies by other authors have focused on preventing woody debris from entering fish passes at their upstream inlet, typically through entrance protection measures such as trash racks or structural deflectors [42–45]. The present approach provides new insights into interior design strategies that can support both ecological functionality and hydraulic soundness**.**

[2] Term baffles was referred to as piers in [41]

2. MATERIALS AND METHODS

2.1. Physical model configuration

Although not directly analyzed, the fish pass adjacent to the Opatowice Weir in Wrocław, Poland (located at river kilometer 245+035 of the Odra River) served as a reference structure for the physical model developed in this study. The Opatowice fish pass is a technical-type bypass channel, divided by a series of cross-walls into ten flow-through chambers. It features a vertical slot configuration, with each cross-wall constructed of five individual baffles, arranged transversely across the channel width.

The physical model used in this study was based on the geometry, baffle layout, spacing, and slope of the Opatowice fish pass. A layout of the baffle arrangement, along with a top-down view and a photograph of the reference structure, is provided in Fig. 1 to aid interpretation.

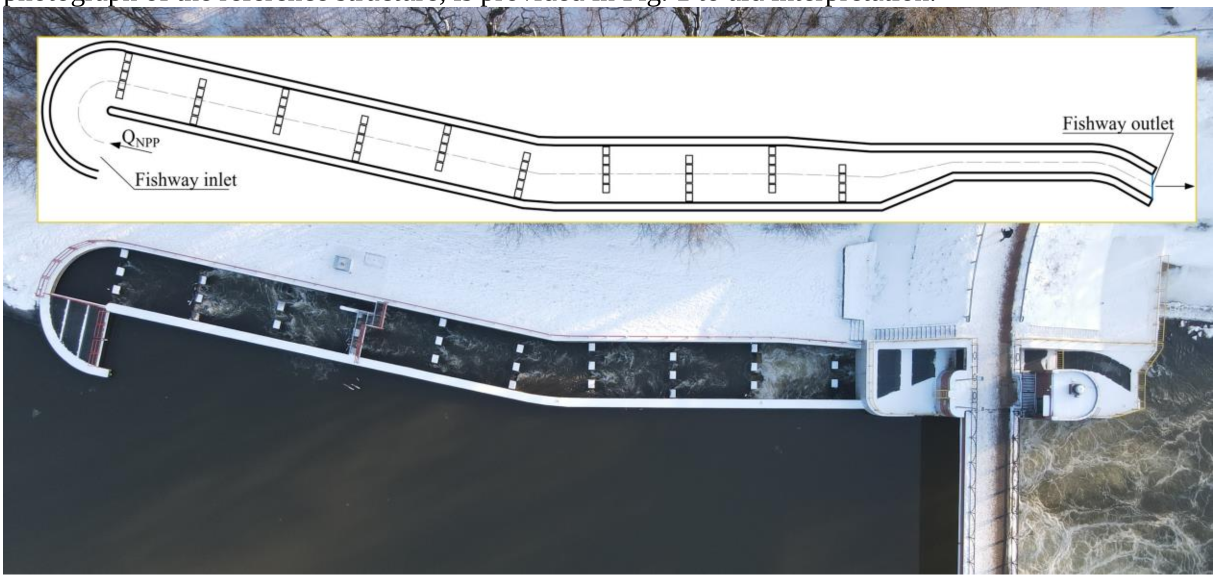

Fig. 1. Top-down drone view of the Opatowice fish pass (Wrocław, Poland) adjacent to the Opatowice Weir, shown with a schematic plan of the vertical-slot configuration used for model reference. The fish pass consists of ten chambers separated by cross-walls containing five baffles each

A more detailed schematic of the fish pass geometry is provided in Fig. 2, showing both the top-down layout of the baffle arrangement and a cross-sectional view of a typical chamber. These technical views illustrate the key spatial relationships between cross-walls and baffles, which were replicated in the physical model.

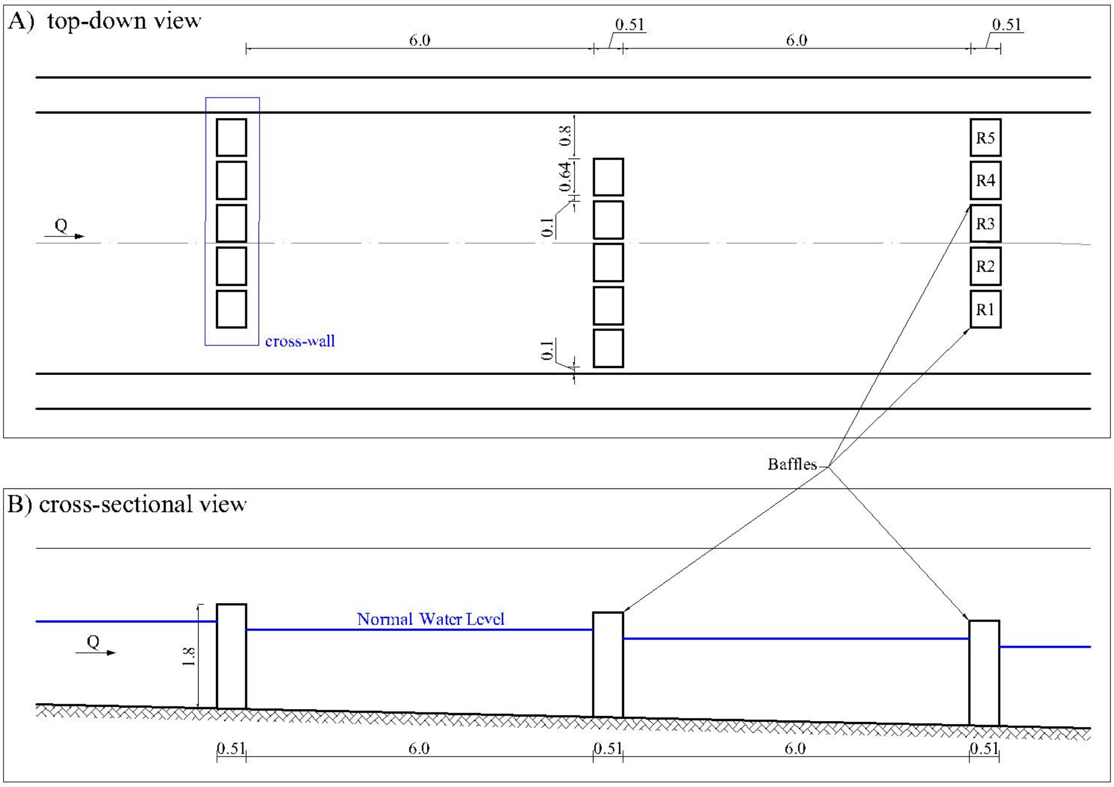

Fig. 2. Representative structural configuration of a single cross-wall in the reference fish pass. (A) Top-down view showing the arrangement of five baffles (R1–R5). (B) Cross-sectional view with main geometric parameters. Arrows indicate flow direction. Units in meters

The baffles are made of concrete and follow a repeated pattern in which three baffles (positions R1, R3, and R5) extend above the water surface, while two (R2 and R4) are fully submerged under typical flow conditions (Fig. 3). This staggered configuration of submerged and emergent elements supports the formation of concentrated flow jets through vertical slots, guiding fish passage under a controlled hydraulic regime.

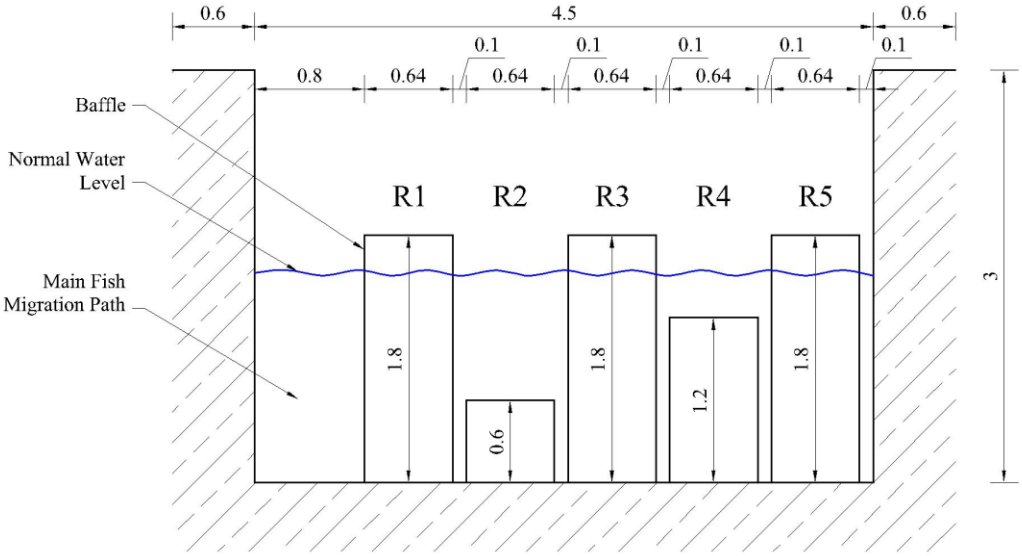

Fig. 3. Cross-section of a reference fish pass cross-wall with alternating emergent (R1, R3, R5) and submerged (R2, R4) baffles. Normal water level (NWL) and main fish migration path indicated. Dimensions in meters

The laboratory physical model was constructed at a geometric scale of 1:50, which was determined based on the available dimensions of the hydraulic flume and the real-world fish pass at the Opatowice Weir. At this scale, the full channel width of the model corresponds proportionally to the width of the actual fish pass.

Given that gravitational forces dominate the hydraulic behaviour of the system, the Froude similarity law[3] was applied for dynamic scaling. Other physical effects, such as viscous or surface tension forces, were assumed negligible. For density [kg·m^{-3}], the Froude number [-] and gravity [m·s^{-2}] the scale is 1:1. Accordingly, the scale factor for linear dimensions is defined as (2.1):

$$\lambda = \frac{L_N}{L_M} = \frac{4{,}5}{0{,}09} = 50[-] \qquad 2.1$$

Where the subscript "N" refers to nature values, and the subscript "M" denotes model values. Based on this, the following scales for other quantities involved in the study are obtained:

- Linear dimensions: 1:50
- Velocity and time: 1:7.07
- Volume and force: 1:125000
- Discharge: 1:17678

Table 1 summarizes the key geometric and hydraulic parameters for both the reference fish pass and the laboratory model:

Table 1. Summary of technical parameters for the reference and laboratory fish pass models

[3] Also referred to as Froude dynamic similarity or Froude scaling law, it ensures that the ratio of inertial to gravitational forces is preserved between the model and the prototype in free-surface flow studies.

Parameter	Scale 1:1	Unit	Model scale 1:50	Unit
Chamber (channel) width	4.5	[m]	90	[mm]
Chamber lenght	6	[m]	120	[mm]
Main slot width	0.8	[m]	16	[mm]
Baffle height (R1/R3/R5 x R2 x R4)	1.8x1.2x0.6	[m]	36x24x12	[mm]
K0 baffle dimensions	0.64x0.50	[m]	12.8x10.0	[mm]
K1 baffle diameter	0.64	[m]	12.8	[mm]
Channel slope	2.20	[%]	2.20	[%]
Discharge[4]	3.85	$[m^3s^{-1}]$	13.1	$[dm^3 \cdot min^{-1}]$
Log length (SW/MW/LW)[5]	0.9/1.35/2.25	[m]	18/27/45	[mm]

A technical drawing of the laboratory model, including the plan view, is presented in

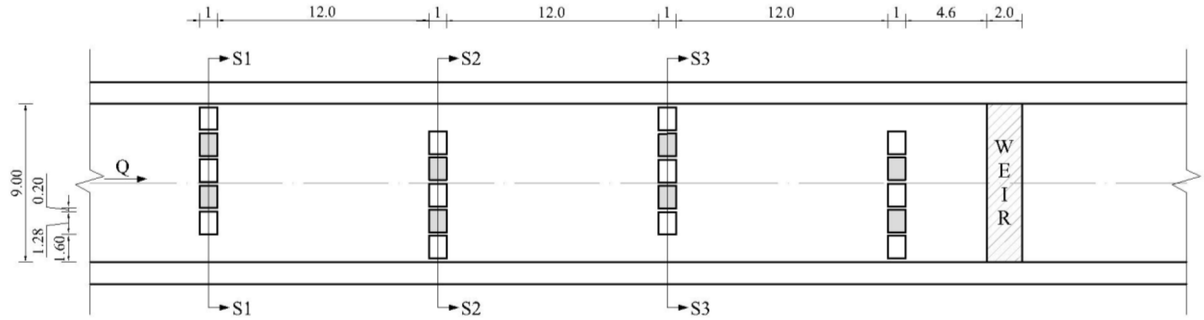

Fig. 4. The model included four cross-walls, three sections and fixed overflow weir.

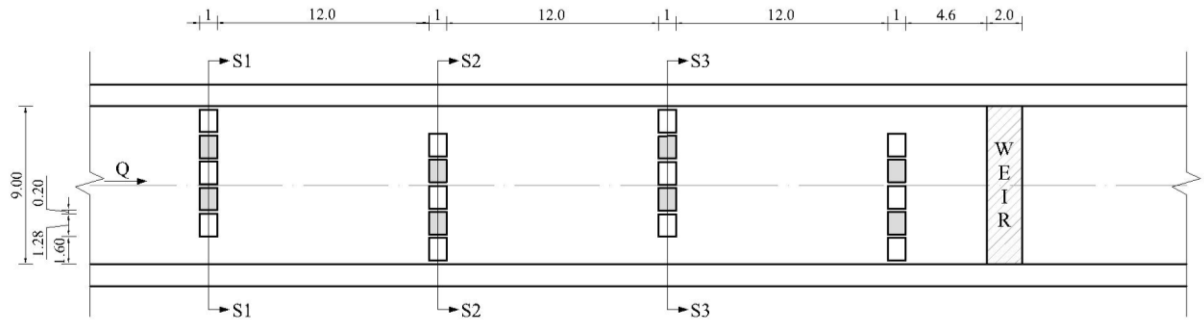

Fig. 4. Plan view of the laboratory fish pass model showing four cross-walls, three sections (S1-S3) and a fixed overflow weir. Each cross-wall contains five baffles, with submerged elements shown in gray. All dimensions in centimeters

Two fish pass configurations were examined in this study, as illustrated in Fig. 5. Configuration K0 corresponds to the unmodified reference structure, in which all emergent baffles (R1, R3, R5) feature a rectangular cross-section. In the modified configuration K1, the shape of these emergent baffles was altered by replacing the original rectangular cross-section with a circular one. The diameter of each circle was equal to the longer side of the original rectangle—i.e., the width of the baffle when viewed from above—resulting in a rounded upstream profile. The modification procedure followed the method described in a previous study [41] and was applied only to the emergent baffles. Submerged baffles (R2,

[4] Discharge, log size classification and corresponding scaled lengths are discussed further in sections.
[5] SW = small wood, MW = medium wood, LW = large wood

R4) were left unchanged in both configurations, as their influence on surface wood accumulation was considered negligible under the tested flow conditions.

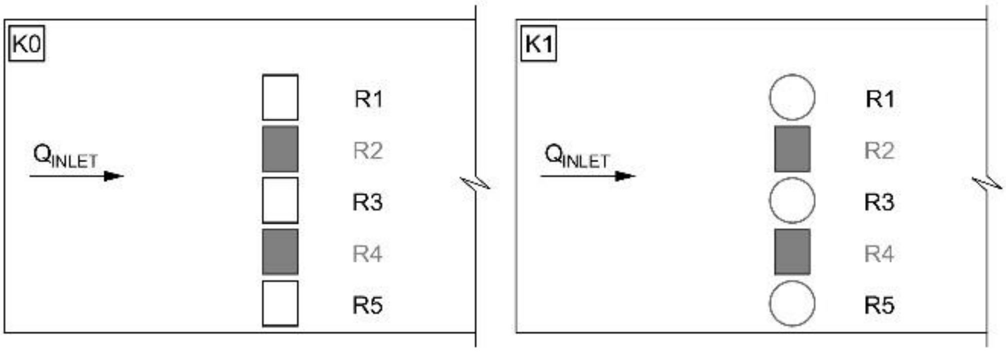

Fig. 5. Comparison of fish pass variants: K0 – original structure with rectangular baffles; K1 – structure with modified emergent baffles (R1, R3, R5). Submerged baffles (R2, R4), shown in gray, remained unaltered in both configurations

To aid interpretation, Fig. 6 presents a schematic illustration of the geometric modification, showing a circle inscribed within a rectangle and highlighting the dimensional equivalence used in the transformation of the baffle cross-section.

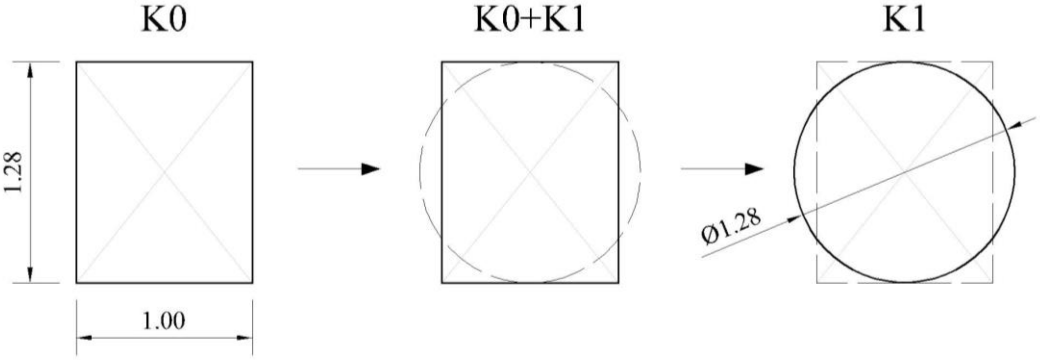

Fig. 6. Transformation of baffle cross-section geometry from the rectangular variant (K0) to the rounded variant (K1). The intermediate step illustrates a circle inscribed in the original rectangle, with the circle diameter equal to the longer side of the rectangle

2.2. Hydraulic conditions

The laboratory experiment was conducted under a single, steady discharge of 13.1 $dm^3 \cdot min^{-1}$, which corresponds—according to Froude similarity scaling—to a flow of 3.85 $m^3 \cdot s^{-1}$ in the reference fish pass. This discharge was selected based on the typical operating conditions of the vertical slot fish pass adjacent to the Opatowice Weir in Wrocław, Poland.

The Opatowice fish pass is integrated into a navigation weir system that ensures a stable impoundment level throughout most of the year. As a result, the hydraulic regime within the fish pass is relatively constant, with limited short-term variability during high-flow events, floods, or ice formation periods [46,47]. The value of 3.85 $m^3 \cdot s^{-1}$ represents the nominal discharge under which the structure normally operates and was therefore adopted as the representative flow condition for the experiment.

The limitation of the study to a single flow scenario was deliberate, as the primary objective was to evaluate the effects of baffle shape**,** log size, and the position of debris retention along the fish pass (i.e., at cross-walls 1, 2, and 3) under consistent and repeatable hydraulic conditions.

2.3. Wood debris design and classification

In this study, wood debris was modeled as a straight cylinder without branches, twigs, or roots, in accordance with the experimental approaches applied in earlier studies [48,49]. Three log length classes were used in the laboratory model:

– Small (SW): 18 mm,
– Medium (MW): 27 mm,
– Large (LW): 45 mm.

All logs had a uniform diameter of 2.8 mm. These model-scale dimensions were derived from a geometric scale of 1:50, and correspond to log lengths of 0.90 m, 1.35 m, and 2.25 m, respectively, in the reference fish pass — equivalent to 20%, 30%, and 50% of the 4.5 m channel width. The logs were made from natural bamboo material, selected for its dimensional consistency, buoyancy, and mechanical stability, which allowed for standardized testing conditions. The detailed parameters of the log classes are presented in Table 2.

Wood was introduced into the flume under uncongested flow conditions, where individual logs were released separately and transported by the current without physical contact. This regime was selected to isolate accumulation mechanisms associated with individual log behavior, avoiding the collective effects observed under congested or semi-congested transport conditions [50].

Table 2. Log parameters (dimensions in millimetres)

Type	Log Length	Log Diameter	Canal width	Log Length/ Canal width	Class
SW	18			0.2	20% flume width
MW	27	2.8	90	0.3	30% flume width
LW	45			0.5	50% flume width

2.4. Experimental design and procedure

The experiment was carried out using a laboratory physical model of a fish pass installed in a flume at the Institute of Environmental Engineering, Wrocław University of Environmental and Life Sciences (Poland). The flume had a rectangular cross-section with internal dimensions of 90 mm width, 310 mm height, and 5000 mm length, and was constructed entirely of transparent acrylic glass [51]. Its adjustable design allowed for slope regulation from –1.21% to 6.70%, and flow rates ranging from 8 to 230 $dm^3 \cdot min^{-1}$.

During the experiment, the flume slope was set to 2.20%, corresponding to the slope of the reference fish pass. The discharge was maintained at 13.1 $dm^3 \cdot min^{-1}$, and monitored using an electromagnetic flowmeter installed on the supply line. A closed-loop system ensured continuous water circulation. To ensure fully developed flow, a flow straightener was installed in the upstream section of the flume.

Although the downstream water level could be adjusted with a sluice gate, this solution did not guarantee stable upstream flow. Therefore, a fixed overflow weir of 20.5 mm height was placed 460 mm downstream of the last cross-wall (see: Fig). This setup ensured a constant water level and steady flow conditions throughout the experiment, which was essential for the reproducibility of the results.

The above elements of the test setup are shown in a photograph of the laboratory installation in Fig. 7.

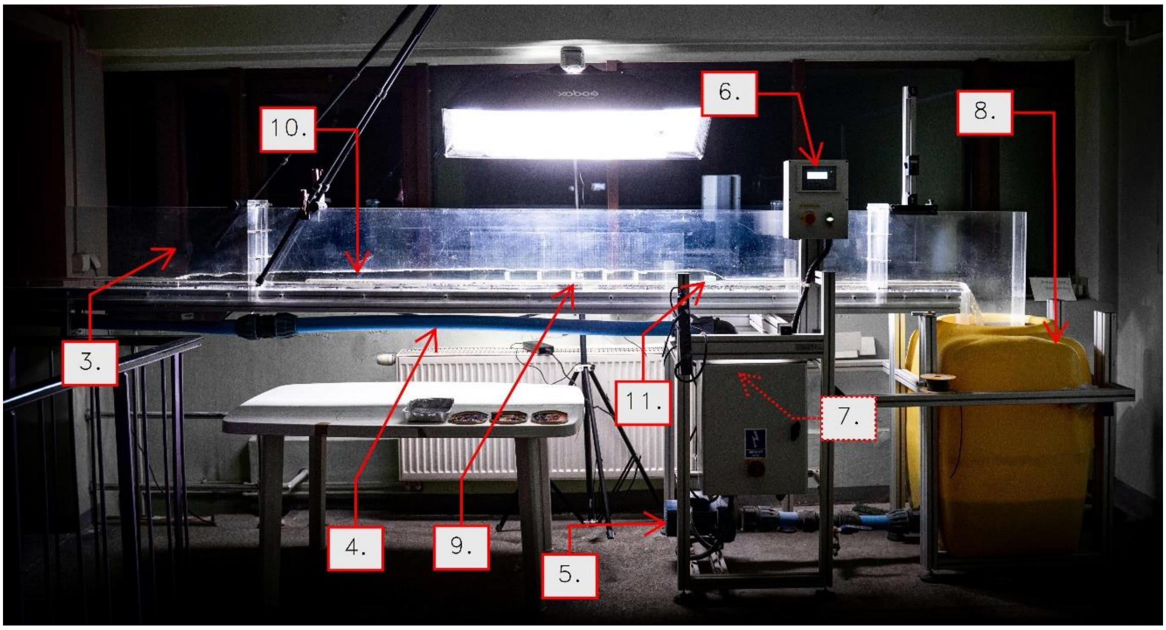

Fig. 7. The laboratory setup. The system includes: (3) Transparent Channel, (4) Inlet Pipe, (5) Hydraulic Pump, (6) Control Panel, (7) Flow Meter (hidden), (8) Closed-Circuit Tank, (9) Fishway Model, (10) Wood Release Point, and (11) Overflow Weir

In accordance with the methodological assumptions, Effective Accumulation measurements were performed at the first three cross-walls (counting in the flow direction). The fourth cross-wall, located at the end of the fish pass, served as a buffer structure to stabilize the flow and shape the upstream hydraulic conditions.

Wood elements were introduced individually into the flow, one every 5 seconds, aligned parallel to the channel axis and flow direction. The insertion point was located approximately 990 mm upstream of the first cross-wall, in a transition zone between supercritical and subcritical flow regimes. This configuration helped increase the randomness of trajectories and better simulate natural conditions.

Prior to each test, the wooden elements were soaked for several minutes to equalize their mass and buoyancy, following established recommendations [49]. A total of 20 logs were introduced per test run, with each test lasting approximately 100 seconds. Each configuration was tested under uncongested transport conditions, and repeated 10 times for each combination of baffle shape (K0, K1) and log size class (SW, MW, LW). In total, 60 tests were conducted, involving the movement of 1200 logs.

The structure of the experimental program is presented in Fig. 8, which outlines the organization of tests with respect to four primary parameters: flow conditions (Q), baffle shape configuration (K), wood size class (S/M/L), and test repetition (T). Each test was assigned a unique identifier, such as K0ST05, denoting the fifth test (T05) using small logs (S), under configuration K0. This naming system ensured unambiguous data management throughout the testing campaign.

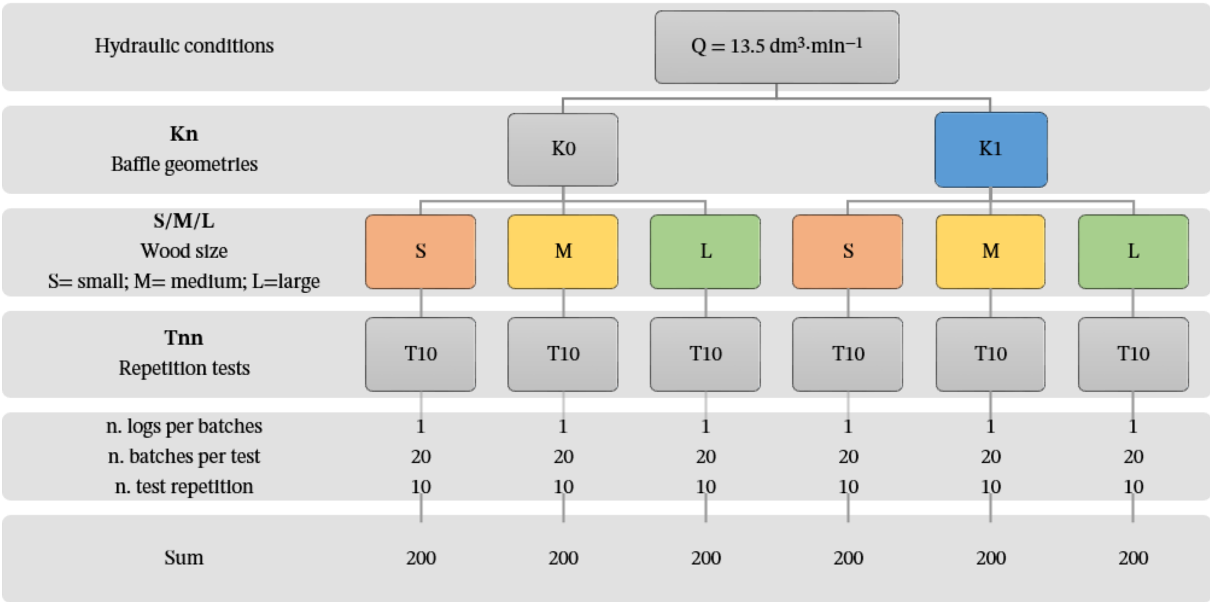

Fig. 8. Diagram illustrating the measurement procedure and experimental test framework

At the end of each test run, the number of retained logs was determined manually by visual inspection. Observations were performed from both sides of the flume, ensuring that all contact points between logs and baffles were clearly visible. Only those logs that were physically lodged against the baffles or visibly influenced by their presence (e.g., held in place by accumulated material around the baffle) were included in the count.

Logs that came to rest between cross-walls without any contact or interaction with a baffle—for instance, those that adhered to the smooth acrylic glass walls due to surface tension or random placement—were treated as outliers and excluded from the analysis.

Importantly, multi-layer accumulations were accounted for. If additional logs were retained as a result of piling onto previously lodged elements, the entire mass was considered part of the blockage. This approach reflects real-world conditions, where log jams typically form as layered structures.

Each test was also video recorded, allowing for post-test review and verification of retention counts in cases of ambiguity or limited visibility during manual inspection.

2.5. Concept of Effective Accumulation

The main response variable in this study was the Effective Accumulation (EA), defined as the ratio between the number of logs retained at the baffles by the end of each test and the total number of logs introduced into the flume (2.2):

$$\mathrm{EA} = \frac{N_{\mathrm{ret}}}{N_{\mathrm{tot}}}\ [-] \tag{2.2}$$

where:

EA – Effective Accumulation, a dimensionless indicator expressing the proportion of introduced wood elements that were retained within the fish pass structure.

N_{ret} – number of wood elements retained at the baffles at the end of a test run.

N_{tot} – total number of wood elements introduced into the flume during a test.

This indicator was calculated for each log size class individually, as well as for all classes combined.

The term *Effective Accumulation* was first introduced by Pina Nicoletta De Cicco in her doctoral dissertation (2017) [48], where it was used to evaluate the accumulation of floating wood around bridge piers of various shapes under controlled laboratory conditions. This indicator has been also used in laboratory studies on wood accumulation around bridge piers [49]. A similar indicator—referred to as *Capture Efficiency*—has been applied in other research [52], defined analogously as the proportion of objects retained relative to the number of elements transported by the flow.

In the present study, EA was calculated individually for each of the three cross-walls (S1–S3), using a stepwise denominator correction approach. Specifically, the number of logs considered as having reached each downstream cross-wall was adjusted to account for prior retention in upstream sections. This correction ensured that the effective accumulation rate at each location reflected only the population of logs actually exposed to that structure, rather than the total number released at the flume inlet.

This method prevents overestimation of downstream retention by applying a conditionally updated denominator, wherein only non-retained logs from previous sections were included in the subsequent analysis.

2.6. Statistical analysis

In this study, a series of statistical analyses was conducted to assess the influence of log length (Size), structure shape (K0 versus K1), cross-wall position (Section), and the interactions between these factors on the value of EA. All analyses were performed in R (version 4.3.2; R Core Team, 2023)[53] using RStudio [54]. Data manipulation and preparation were carried out using the dplyr [55] and tidyr [56] packages, while plots were generated using ggplot2 [57]. Statistical testing involved the use of FSA [58] for Dunn's post hoc tests, and ARTool for nonparametric factorial analysis via the aligned rank transform [59–61]. Base R functions from the stats package were used for classical parametric and nonparametric tests, including Shapiro-Wilk, Wilcoxon, and ANOVA [62] procedures.

The normality of the dependent variable distribution was assessed using the Shapiro-Wilk test [63], performed separately for each combination of grouping variables. As the assumption of normality was not met in the majority of the cases, nonparametric tests were chosen as the primary analytical tools. The effect of log length (Size) on Effective Accumulation within each structure shape variant (K0 and K1) was evaluated using the Kruskal-Wallis test [64], followed by Dunn's test with Bonferroni correction [65] to identify significant pairwise differences. Comparisons between the two structural shapes were made using the Wilcoxon rank-sum test [66], performed globally and separately within each size class. To investigate potential interactions between baffle shape and cross-wall position, a factorial analysis was carried out for each log size class using the aligned rank transform (ART). In parallel, a classical two-way ANOVA with Tukey's HSD post hoc test [67] was also conducted to support and compare results under parametric assumptions.

The primary response variable in all analyses was EA, defined as the proportion of logs retained at each cross-wall, adjusted for upstream retention as described in Section 2.5. For statistical comparison between test series, the mean value across the three cross-walls was used and denoted as EA_total. This allowed comparisons to focus either on local retention behavior (EA) or on overall structural performance (EA_total), depending on the analytical objective. All visualizations presented in the results section were constructed using ggplot2 [57] and include group means with standard errors to support statistical interpretations.

3. RESULTS

3.1. Influence of Log Size on Effective Accumulation

One of the central aims of this study was to determine how log length influences the effectiveness of debris retention in a vertical-slot fish pass. Given that wood debris varies considerably in size under natural conditions, understanding how different length classes behave in contact with structural elements is essential for designing fish passes that minimize internal blockage.

To assess this, EA_total was compared between log size classes (SW, MW, LW) within each baffle geometry variant (K0 and K1). The Shapiro-Wilk test for EA_total indicated that this response variable was normally distributed for all sizes of K0 and normally distributed for sizes LW and SW of K1, but non-normal for MW of K1 (Table 3). Additionally, the Shapiro-Wilk test for combined EA_total distributions indicated non-normality for both K0 ($W = 0.870$, $p = 0.002$) and K1 ($W = 0.853$, $p = 0.001$). Based on these findings, nonparametric procedures were prioritized for the comparison of log size classes, with one-way ANOVA applied in parallel to validate the robustness of the results

Table 3. Shapiro-Wilk test results for EA_total by shape and size class

Shape	Size	***n***	***p*-value**	Normality
K0	LW	10	0.422	YES
K0	MW	10	0.766	YES
K0	SW	10	0.308	YES
K1	LW	10	0.346	YES
K1	MW	10	0.048	NO
K1	SW	10	0.283	YES

Due to deviations from normality observed in some log size–shape combinations, the Kruskal-Wallis test was applied separately for each baffle shape to examine differences in EA_total among the three log size classes. The results indicated statistically significant differences in effective accumulation between size classes for both structural configurations. For the rectangular baffles (K0), the test yielded $\chi^2 = 25.19$ with a p-value < 0.001, while for the rounded baffles (K1), the result was $\chi^2 = 23.06$, also with a p-value < 0.001. These findings confirm that log size had a significant effect on EA_total regardless of baffle geometry (Table 4).

Table 4. Kruskal-Wallis test results for EA_total by log size class

Shape	χ^2 (df = 2)	***p*-value**	Significance[6]
K0	25.19	3.38×10^{-6}	***
K1	23.06	9.83×10^{-6}	***

Pairwise comparisons between log size classes were performed using Dunn's test with Bonferroni correction, separately for each structure shape. The results are presented in **Błąd! Nieprawidłowy odsyłacz do zakładki: wskazuje na nią samą.**. Significant differences were observed between the largest (LW) and smallest (SW) logs for both shapes ($p < 0.00001$), as well as between LW and MW ($p = 0.028$ for K0; $p = 0.013$ for K1). A significant difference between MW and SW was found only for the rectangular baffles (K0, $p = 0.047$), while no significant difference was observed for the rounded baffles (K1, $p = 0.169$).

[6] For symbol explanation, see Table A in the Additional Information section

Table 5. Dunn's post hoc test results (adjusted *p*-values)

Shape	Comparison	*p*-value	Significance
K0	LW – MW	0.028	*
K0	LW – SW	<0.00001	***
K0	MW – SW	0.047	*
K1	LW – MW	0.013	*
K1	LW – SW	<0.00001	***
K1	MW – SW	0.169	—

To complement the nonparametric analysis, a one-way analysis of variance (ANOVA) was also performed separately for each structural shape to compare EA_total across log size classes. Despite a minor deviation from normality observed in the K1-MW group ($p = 0.048$), the overall distribution was close to normal. Furthermore, ANOVA is considered robust to moderate violations of normality, especially in balanced designs with equal sample sizes [68,69].

The results of the ANOVA tests are shown in Table 6. For both structural variants, the differences in EA_total among the three log size classes were highly significant. Specifically, the *F*-tests yielded large F values (84.46 for K0 and 88.11 for K1), with corresponding *p*-values of 2.4×10^{-12} and 1.46×10^{-12}, respectively, confirming a strong effect of log length on retention efficiency in both configurations

Table 6. ANOVA results for EA_total by log size class

Shape	df (between)	*F* value	*p*-value	Significance
K0	2	84.46	2.4×10^{-12}	***
K1	2	88.11	1.46×10^{-12}	***

Following the ANOVA, Tukey's HSD post hoc test was applied to identify significant differences between specific size classes. As shown in Table 7. all comparisons involving the longest logs (LW) were statistically significant ($p < 0.00001$) for both K0 and K1, confirming that large logs accumulate more effectively than shorter ones. For K0, the difference between SW and MW was also significant ($p = 0.006$), indicating a progressive increase in EA_total with log length. In contrast, under K1, the SW–MW comparison was not significant ($p = 0.080$), suggesting that accumulation remained similarly low for both shorter classes in this configuration.

Table 7. Tukey HSD test results (adjusted *p*-values)

Shape	Comparison	*p*-value	Significance
K0	MW – LW	<0.00001	***
K0	SW – LW	<0.00001	***
K0	SW – MW	0.006	**
K1	MW – LW	<0.00001	***
K1	SW – LW	<0.00001	***
K1	SW – MW	0.080	.

These findings are visualized in Fig**.** 9, which displays the mean values of EA_total for each log size class grouped by baffle shape. The tallest bars correspond to LW logs, especially under K0, where accumulation exceeded 0.4. Under K1, a similar trend is observed, though at a slightly lower magnitude. MW logs showed intermediate values under both shapes, while SW logs consistently resulted in the lowest retention. Error bars represent standard errors. Compact letter display (CLD) [7] is used to indicate statistically significant differences between groups within each shape.

[7] Compact letter display (CLD) is a graphical method for denoting statistically homogeneous groups in post-hoc tests such as Tukey's HSD. Groups sharing the same letter (e.g., "A") are not significantly different, whereas different letters (e.g., "A" vs. "B") indicate significant differences at $P < 0.05$ [100]

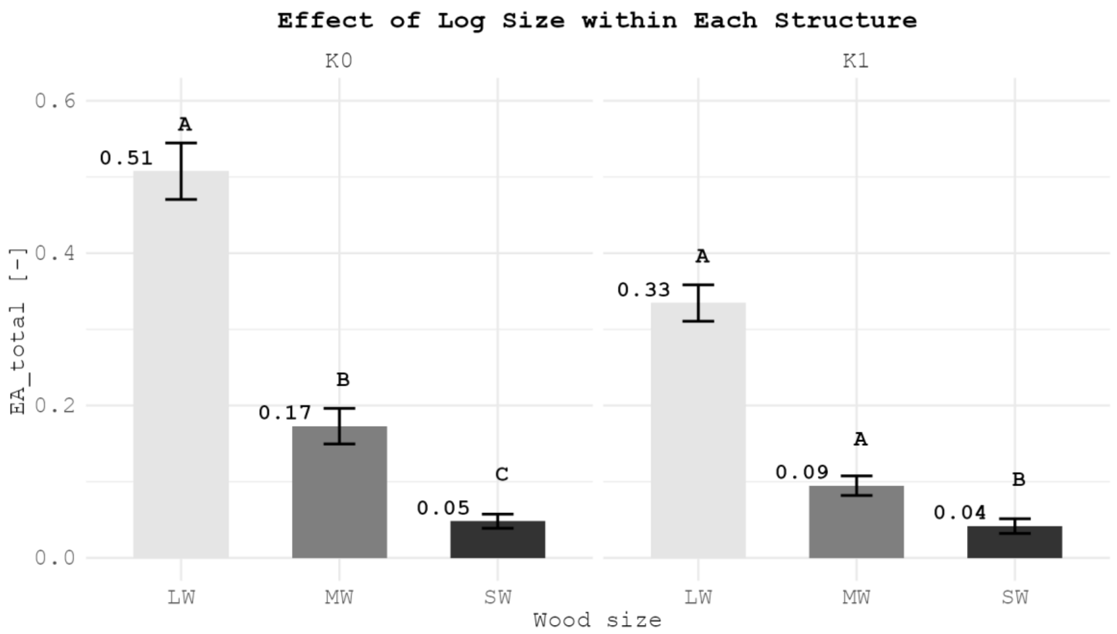

Fig. 9. Effect of log size on Effective Accumulation (EA_total) for two baffle shape variants (K0 and K1). Bars represent mean values; error bars indicate standard error of the mean. Different uppercase letters (A, B, C) indicate statistically significant differences between size classes within each baffle shape

3.2. Comparison of Baffle Shapes Within Each Log Size Class

Differences in EA_total between the two baffle shapes were examined separately for each log size class to identify potential interactions between geometry and wood length. The results of the ART analysis are summarized in Table 8 and indicate that the effect of baffle shape on EA_total varied across log size classes. For small logs (SW), no significant difference was observed between the two baffle types (p = 0.475), suggesting that geometry had limited impact on the accumulation of short debris. In contrast, for both medium (MW) and large logs (LW), the effect of shape was statistically significant (p = 0.012 and p = 0.009, respectively), with rectangular baffles (K0) demonstrating higher retention rates. These findings suggest that shape plays a critical role in facilitating accumulation for longer wood elements.

Table 8. Results of the Aligned Rank Transform (ART) analysis by log size class

Size Class	Effect	*F*	*p*-value	Significance
SW	Shape	0.52	0.475	—
MW	Shape	6.69	0.012	*
LW	Shape	7.26	0.009	**

These trends are visually illustrated in Fig. 10, which presents the mean EA_total values for small (SW), medium (MW), and large (LW) logs, grouped by baffle shape. Bars represent group means, and vertical lines indicate standard error of the mean. For small logs, accumulation levels were low and similar between the two configurations (K0 = 0.05, K1 = 0.04). For medium logs, accumulation was higher in K0 (0.17) than in K1 (0.09), indicating moderate influence of geometry. For large logs, the difference was most pronounced, with K0 yielding 0.51 and K1 yielding 0.33. These patterns suggest that the influence of baffle shape becomes increasingly important with log size.

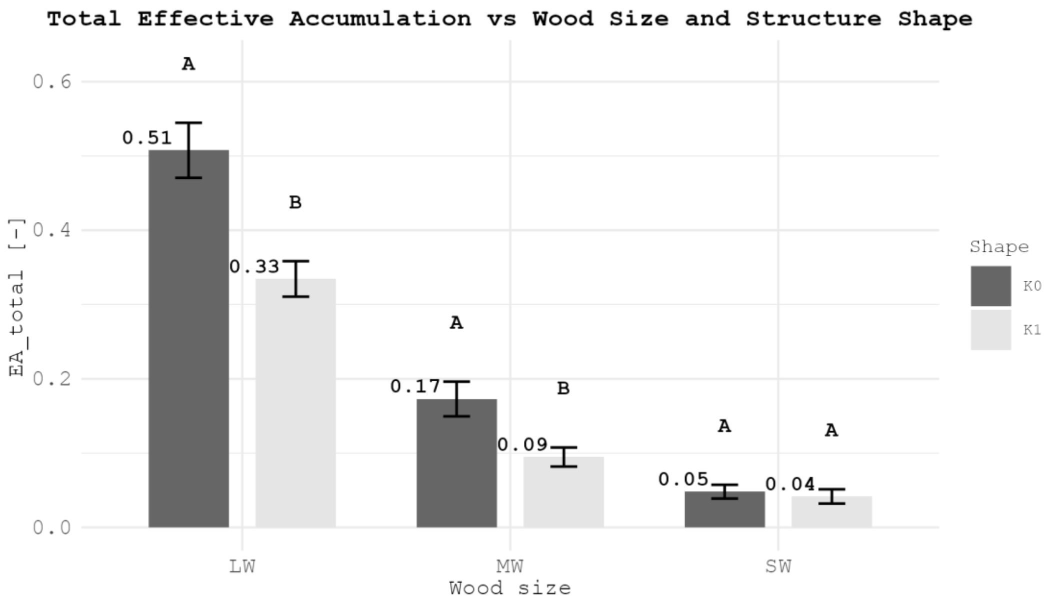

Fig. 10. Comparison of Effective Accumulation (EA_total) between rectangular (K0) and rounded (K1) baffles within each log size class. Bars represent mean values; error bars indicate standard error of the mean. Different uppercase letters (A, B, C) indicate statistically significant differences between size classes within each baffle shape

To support the findings from the ART analysis, a classical two-way ANOVA was conducted for each log size class. The results aligned closely with the nonparametric outcomes. For small logs (SW), no significant effect of baffle shape was observed ($p = 0.647$), and there was no significant interaction between shape and section. However, a significant effect of section ($p = 0.013$) indicated spatial variability in retention that was independent of geometry. For medium logs (MW), the effect of shape was statistically significant ($p = 0.014$), with rectangular baffles (K0) retaining more wood than rounded ones (K1). The interaction term approached significance ($p = 0.081$), suggesting a potential location-dependent influence of shape, while section alone had no discernible effect.

For large logs (LW), both baffle shape ($p = 0.009$) and section ($p < 0.001$) had statistically significant effects on EA_total, indicating that both geometry and spatial position strongly influenced accumulation. No significant interaction was observed ($p = 0.145$).

Overall, these results validate the outcomes of the ART analysis and reinforce the conclusion that baffle shape has a measurable effect on the retention of medium and large wood, with rectangular configurations supporting higher levels of accumulation.

3.3. Spatial Distribution of Effective Accumulation Across Cross-Walls

This section presents the distribution of effective accumulation (EA) across the first three cross-walls (S1–S3) of the fish pass model, based on aggregated values from all log length classes (SW, MW, LW). The results are shown separately for the two baffle configurations: rectangular (K0) and rounded (K1), providing a general overview of retention efficiency throughout the structure.

Fig. displays the mean EA values with standard errors, grouped by baffle shape and cross-wall location. For rectangular baffles (K0), the highest EA occurred at S1 (0.31), followed by a decrease at S2 (0.18) and a moderate increase at S3 (0.23). Rounded baffles (K1) exhibited consistently lower EA values, decreasing from 0.24 (S1) to 0.16 (S2) and further to 0.07 (S3).

These raw patterns suggest that rectangular baffles were generally more effective in retaining wood at each cross-wall, with the most noticeable difference observed at S3 (0.23 for K0 vs. 0.07 for K1). However, because this visualization does not account for statistical significance, formal inference is presented in the following subsection, based on Aligned Rank Transform (ART) analysis.

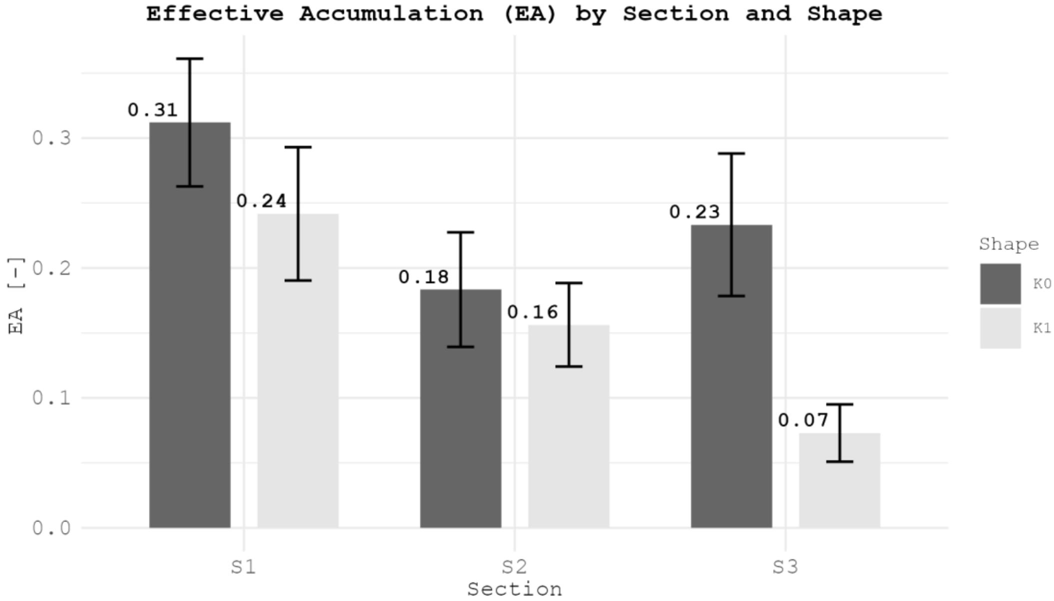

Fig. 11. Mean effective accumulation (EA) across the first three cross-walls (S1–S3) for baffle shapes K0 (rectangular) and K1 (rounded). Results are aggregated across all log length classes. Error bars represent standard errors

To determine whether spatial differences in wood accumulation were statistically significant between baffle configurations and cross-wall positions, a factorial analysis was performed using the Aligned Rank Transform (ART), followed by a classical two-way ANOVA for validation. Both models included the fixed effects of baffle shape (Shape), cross-wall location (Section), and their interaction (Shape × Section). Unlike in Section 3.2, the analysis here was based on data aggregated across all log size classes to provide a generalized view of retention behaviour.

The ART results revealed statistically significant main effects for both Shape and Section. Rectangular baffles (K0) were associated with higher overall EA values compared to rounded baffles (K1) ($F(1,174) = 3.73$, $p = 0.055$), although this effect was marginal. The effect of Section was statistically significant ($F(2,174) = 4.13$, $p = 0.018$), indicating log accumulation differed among cross-section location. The interaction term (Shape × Section) was not significant ($p = 0.191$), suggesting that the effect of baffle shape was consistent across spatial positions. The ART results are summarized in Table 9:

Table 9. Results of the Aligned Rank Transform (ART) ANOVA for the effects of baffle Shape, cross-wall Section, and their interaction on Effective Accumulation (EA), based on aggregated data (SW, MW, LW)

Effect	df	Residual df	*F*	*p*-value	Significance
Shape	1	174	3.73	0.055	·
Section	2	174	4.13	0.018	*
Shape × Section	2	174	1.67	0.191	—

The classical two-way ANOVA produced results consistent with the nonparametric ART analysis. Although the assumption of normality was not met in several groups (as indicated by the Shapiro-Wilk test), the ANOVA confirmed the significance of both Shape and Section, while also reporting no significant interaction. This agreement between parametric and nonparametric approaches strengthens the reliability of the observed effects.

To explore the source of the significant Section effect, post-hoc pairwise comparisons were conducted using aligned rank transformed data. These tests assessed whether effective accumulation differed significantly between the three cross-wall positions (S1, S2, S3), irrespective of baffle geometry.

The results revealed that the difference between S3 and S1 was statistically significant ($p = 0.009$), indicating lower retention efficiency in the final cross-wall (S3). The contrasts between S1 and S2 ($p = 0.17$) and between S2 and S3 ($p = 0.48$) were not significant. These findings suggest that the initial cross-wall (S1) retained more debris than the final one, with S2 showing intermediate values. The statistical outcomes are summarized in Table 10.

Table 10. Pairwise comparisons of effective accumulation (EA) between cross-wall sections based on aligned rank transformed data

Comparison	Estimate	SE	*z*-value	*p*-adj	Significance
S2 – S1	-16.575	9.217	-1.798	0.173	—
S3 – S1	-27.300	9.217	-2.962	0.009	**
S3 – S2	-10.725	9.217	-1.164	0.476	—

To further illustrate the differences between sections, Fig. presents the average EA values across S1, S2, and S3, aggregated across all log size classes and baffle shapes. The plot highlights that first cross-wall (S1) retained the most debris, followed by a substantial drop in S2, and a further decline in S3. Although only the S1–S3 comparison reached statistical significance, the visual trend supports the interpretation of a gradual reduction in retention efficiency along the fish pass.

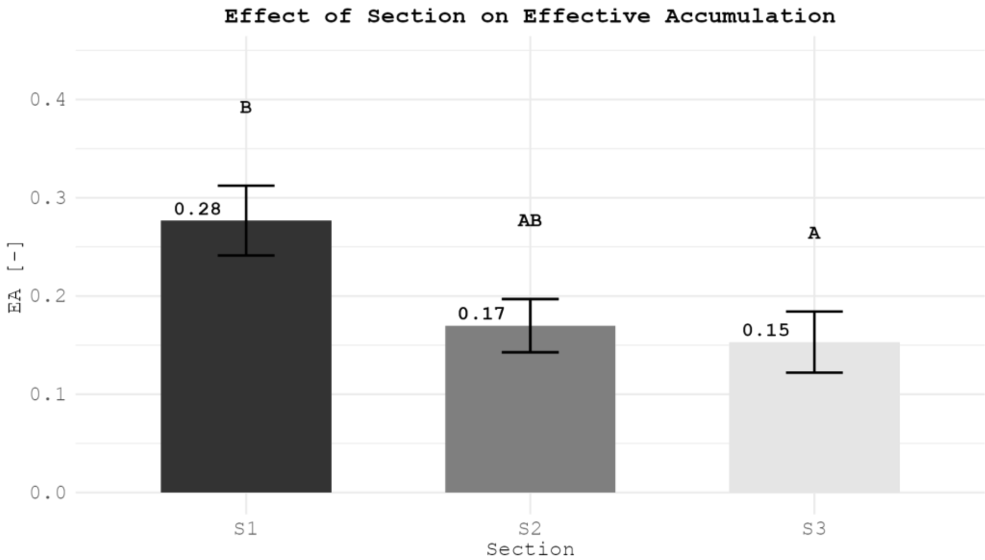

Fig. 12. Effective accumulation (EA) across cross-wall sections (S1–S3), aggregated across all log size classes and baffle shapes. Bars represent mean values with standard errors. Statistically significant differences were found only between S1 and S3 ($p < 0.01$), indicating reduced retention efficiency toward the downstream end of the fish pass. Different uppercase letters (A, B, C) indicate statistically significant differences between size classes within each baffle shape

3.4. Total Effective Accumulation of wood

This section presents a synthetic comparison of the two tested baffle configurations—rectangular (K0) and rounded (K1)—in terms of their overall ability to retain wood. The analysis was based on the total Effective Accumulation (EA_total), defined as the average proportion of logs retained across all cross-walls (S1–S3) and all wood size classes (SW, MW, LW). This global metric provides a simplified overview of the structural performance under uniform hydraulic conditions and uncongested debris transport.

The mean EA_total for rectangular baffles (K0) was 0.24, compared to 0.16 for rounded baffles (K1), suggesting a higher average accumulation in the former configuration (see: Fig.). However, this apparent difference was not supported by statistical inference.

To assess significance, a nonparametric Wilcoxon rank-sum test was conducted, as the normality assumption was violated for both groups (Shapiro-Wilk test: $p = 0.002$ for K0, $p = 0.001$ for K1). The Wilcoxon test yielded a p-value of 0.151 (W = 547.5), indicating that the observed difference in EA_total between configurations was not statistically significant.

It is important to note that this total accumulation analysis does not account for key sources of variability, such as log size or cross-wall location, which were found to influence accumulation in previous sections. As such, this test has limited explanatory power, and the observed difference should be interpreted with caution.

Despite these limitations, the results are included here as a complementary perspective. The aggregated comparison may offer a visual reference of general tendencies in retention behavior, even if not statistically conclusive.

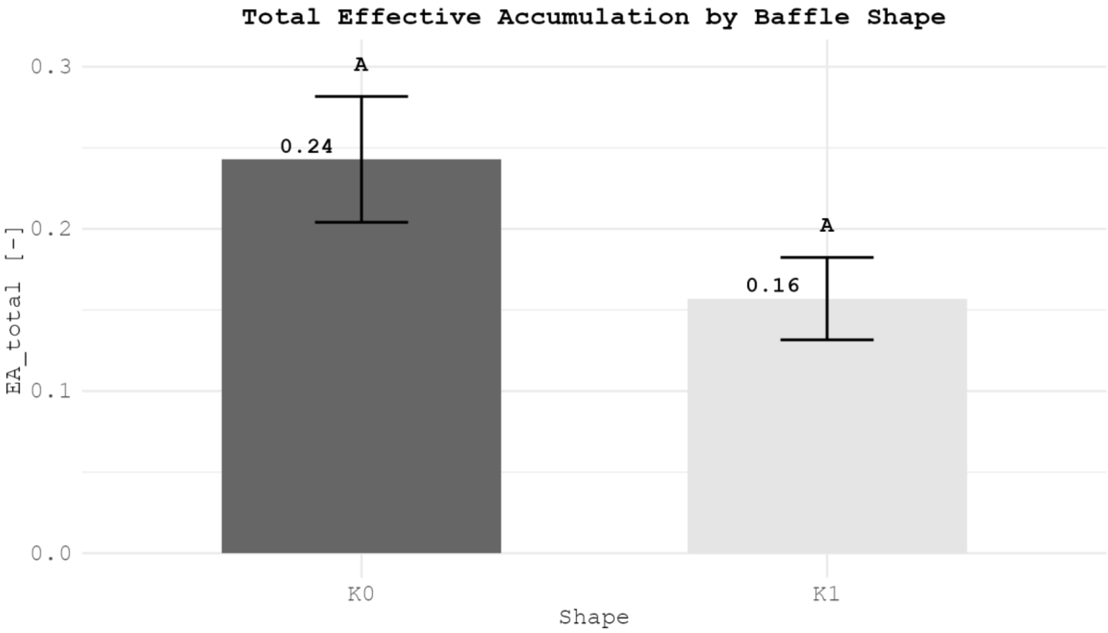

Fig. 13. Total Effective Accumulation (EA) for rectangular baffles (K0) and rounded baffles (K1), calculated across all wood size classes and cross-wall sections. Bars represent means; error bars indicate standard errors. The difference was not statistically significant (Wilcoxon test, $p = 0.151$), and the analysis does not account for variability due to log size or spatial position

To verify whether this observed difference was statistically significant, a Wilcoxon rank-sum test was applied. Prior to testing, the normality of EA_total distribution for each shape was assessed using the Shapiro-Wilk test. Despite the visual difference in EA_total between baffle shapes, the observed difference was not statistically significant. A Wilcoxon rank-sum test, applied due to deviations from normality, yielded a p-value of 0.151 (W = 547.5), indicating no significant difference in total accumulation between the two configurations under the tested conditions.

Normality checks using the Shapiro-Wilk test revealed that EA_total values for both K0 and K1 deviated significantly from a normal distribution (p = 0.002 and p = 0.001, respectively). As a result, the nonparametric Wilcoxon test was considered appropriate. While the rectangular configuration showed higher mean accumulation (0.24 vs. 0.16), the difference was subject to high variability and should not be interpreted as statistically robust.

4. DISCUSSION

This study provides new insights into how the geometry of internal baffles in vertical slot fish passes affects the accumulation of woody debris. By isolating the effects of structural shape, debris size, and spatial position within the structure, the experiment allowed for a detailed analysis of interactions that influence the risk of internal blockage under controlled flow conditions.

The findings confirm that modifying the baffle shape from rectangular (K0) to rounded (K1) affects debris retention patterns in meaningful ways. While the total Effective Accumulation (EA_total) across all classes and sections was not significantly different between the two configurations, significant effects emerged when the data were disaggregated. Specifically, differences in accumulation were strongly influenced by log size and cross-wall position, indicating that global performance metrics may obscure important local behaviors within the fish pass.

These results mark a preliminary yet important step in the design-based evaluation of fish pass resilience to natural floating material, building upon earlier findings from bridge engineering [43,46] and expanding them to the context of ecological infrastructure.

One of the key findings of this study is the strong influence of log length on debris accumulation within fish pass chambers. The results clearly demonstrate that Effective Accumulation (EA) increases with log size, regardless of baffle shape. This trend was consistently observed in both statistical frameworks (Kruskal-Wallis, ANOVA) and across both structural variants (K0 and K1), confirming that larger elements are significantly more prone to retention under the tested conditions.

While small wood (SW) exhibited minimal accumulation in both configurations, particularly in K1, medium (MW) and especially large logs (LW) were retained more frequently—highlighting a clear size-dependent accumulation pattern. The highest average EA_total was observed for LW in K0 (0.51), followed by K1 (0.33), confirming that baffle shape further amplifies size-dependent effects. Interestingly, the difference between MW and SW was not statistically significant in K1, suggesting that smoother geometry reduces size selectivity.

The analysis of effective accumulation versus log length (Fig) indicates that EA increases with log size, regardless of baffle shape. However, for each size class, rectangular baffle (K0) exhibited a higher capacity to trap wood than rounded baffles (K1). A minor difference in retention efficiency was noted for SW between K0 and K1, though rectangular baffles K0 slightly more frequently retained these small elements. Small logs are less susceptible to specific flow disturbances generated by differences in baffles geometry. The sharp angle changes in the flow around K0 baffles can create more pronounced stagnation zones, whereas rounded baffles (K1) induce smoother flow curvature. The results suggest that this factor is less influential for small elements. Therefore, small logs, which float easily and follow the main current, exhibit smaller differences (ΔEA=0.01) in accumulation between baffle shapes.

A comparable phenomenon is observed in Particle Image Velocimetry (PIV), where small tracer particles are used to track flow movement. Their small size allows them to accurately replicate flow trajectories, minimizing inertia effects and interactions with local disturbances [70,71]. Similarly, small logs in the fish pass follow the primary flow path and exhibit a lower tendency to become trapped compared to larger elements.

Some researchers [52] suggest that under subcritical flow conditions, the shape of obstacles and debris can affect trapping efficiency—higher flow rates and smaller debris pieces favor reduced blockage formation. This aligns with observations for small logs (SW), which show a lower tendency for accumulation compared to larger wood elements.

Longer logs (MW and LW) demonstrated a higher tendency to become trapped within the fish pass chambers. Due to their length, they can interact simultaneously with multiple baffles, which promotes retention. They create a "bridge effect" between structural elements, hindering further transport. Additionally, their greater length and mass make them less susceptible to rapid changes in flow direction. When their ends reach low-velocity zones, they are more likely to become "trapped," as their higher inertia prevents reorientation and re-entry into the main flow.

According to potential flow theory [72], pier (or baffle in this case) geometry influences the shape and curvature of flow paths. For sharp-edged baffles (K0), flow paths may create more pronounced stagnation zones, favoring wood retention. Longer logs occupy a larger space, increasing the probability of interaction with these zones and thus raising the risk of blockage. Flow paths around the baffles differ in curvature – for rectangular piers (in our case K0 baffle shape), the angle of flow deflection relative to the main current is approximately 85°, whereas for rounded piers (in our case K1 baffle shape), it is about 45° [49]. For smaller logs, these differences in deflection angles are less significant, as their movement is more governed by the main flow.

The comparison of EA_total values between rectangular (K0) and rounded (K1) baffle shapes within each log size class confirmed that baffle geometry plays a significant role in the retention of medium and large wood elements, but not for small ones. This was supported both visually (Fig. 1) and statistically, as significant differences between K0 and K1 were observed for MW and LW classes, while no significant difference was detected for SW logs.

The lack of shape effect in the SW class can be attributed to the short length of these logs (18 mm, 20% of channel width), which makes them less likely to interact physically with baffles. Their reduced cross-sectional reach likely results in a low probability of collision, regardless of structural geometry. This observation aligns with findings from bridge pier studies, where the retention probability of wood was shown to increase sharply with log length [49].For medium and large logs, rectangular baffles consistently produced higher accumulation rates. This is likely due to their sharper corners and larger upstream face, which facilitate the direct blocking or wedging of debris. Rounded baffles, in contrast, appear to promote smoother flow transitions and reduce areas where debris can lodge.

The significant difference in EA_total for LW logs (0.51 for K0 vs 0.33 for K1) further highlights the importance of geometric features in managing internal debris accumulation. As larger logs are more likely to span across flow paths and contact multiple baffles simultaneously, they are also more sensitive to changes in the upstream profile of the obstruction.

Interestingly, the interaction effects between baffle shape and cross-wall location (Shape × Section) were not statistically significant for any log size class. This indicates that the effect of baffle geometry is consistent along the fish pass, and not localized to a specific area. This consistency may reflect the stable hydraulic regime used in the experiments, where flow conditions were held constant throughout the structure.

These findings provide strong evidence that baffle shape modifications can reduce internal blockage by longer debris, while having minimal impact on the passage of small wood. This has practical implications for fish pass design: rounded baffles may help maintain hydraulic performance and ecological connectivity without significantly increasing the risk of debris accumulation, at least for small to medium wood input.

Overall, these results confirm that log length is a dominant factor influencing accumulation probability under non-congested transport conditions, and that geometric features of internal structures significantly affect how debris interacts with the flow environment.

In addition to debris size and structure shape, the spatial location of retention within the fish pass plays an important role in understanding how and where blockages form. Effective Accumulation (EA) was analyzed separately for each cross-wall (S1, S2, S3), allowing a spatial interpretation of debris trapping patterns along the structure. This was performed using cumulative measurements across all log sizes.

Statistical analysis confirmed a significant main effect of cross-wall location on wood retention (p = 0.018, ART), with distinct accumulation profiles observed for the two structural configurations. While rectangular baffles (K0) showed a non-monotonic EA pattern (high–low–medium), rounded baffles (K1) exhibited a clear decreasing trend from upstream to downstream.

The experiment followed a system in which 20 logs were introduced into the flume at 5-second intervals, and EA was calculated as the ratio of the number of logs retained in a given cross-section to the number of logs that had not been trapped in the upstream sections. The analysis of EA across successive cross-sections, regardless of log size, enabled the identification of general trends in wood accumulation within the fish pass. It is worth noting that the present analysis focused on the first three cross-walls of the fish pass model, which were selected based on consistent flow conditions and measurement comparability. In the context of future research directions, a separate experimental variant was explored in which the number of measuring cross-sections was increased to five. While the findings from that investigation are not included in the present study, they are currently being developed in collaboration with an external research team as part of an independent project.

The observed differences in EA for various baffles geometries indicate that the structural design significantly influences the spatial distribution of wood retention. The decreasing EA trend observed for rounded baffles (K1) across successive sections (EA values: 0.24 → 0.16 → 0.07) may reflect smoother wood transport through the fish pass. In contrast, rectangular baffles (K0) exhibited an irregular EA distribution (0.31 → 0.18 → 0.23), suggesting the presence of local hydrodynamic effects, such as velocity variations within the fish pass chambers. This behavior may be associated with a different velocity distribution pattern, as the rectangular-baffle configuration tends to form more pronounced resting zones for fish.

Another factor influencing wood accumulation in the fish pass is the "snowball effect". There is a high probability of wood being retained in the first measurement section, as it represents the initial opportunity for logs to interact with an obstacle. As accumulation progresses, the probability of subsequent logs becoming trapped increases, as they can be retained not only by the structural baffles but also by previously lodged elements. As a result, this process can lead to the self-reinforcing growth of blockages, driven by additional accumulating elements (Fig.).

Similar material accumulation processes are observed across various scientific and engineering disciplines, where the buildup of elements in flow gradually restricts further movement. This mechanism is widely studied in the context of woody debris transport in river systems [22,73], as well as in other physical processes [74] or even psychology [75].

In scientific literature, this phenomenon is referred to as the "jamming phenomenon," which describes the transition of a system of particles from a free-flowing state to a jammed, immobilized state due to increased density or spatial constraints [76,77]. This effect occurs in various contexts, including traffic congestion, granular material flow, and biological systems. In hydraulic engineering and riverine ecology, this process manifests as log-jamming, where retained logs form structures that obstruct the flow of water and additional debris.

This mechanism is also utilized in Engineered Log Jams (ELJs), which are designed to stabilize riverbanks, improve water quality, and enhance aquatic habitats by mimicking natural wood accumulation processes [78–81]. ELJs influence flow patterns, sediment transport, and riverbed morphodynamics, contributing to increased hydraulic diversity and providing fish refuges [78–81].

In the context of this study, the jamming effect was particularly evident for large logs (LW), which, as blockages grew, were no longer retained directly by the baffles but rather by previously trapped elements, amplifying the accumulation process. The resulting structure resembles well-known jamming and clogging mechanisms [22], confirming that initial wood-obstacle interactions can be crucial in shaping the subsequent development of blockages within the fish pass.

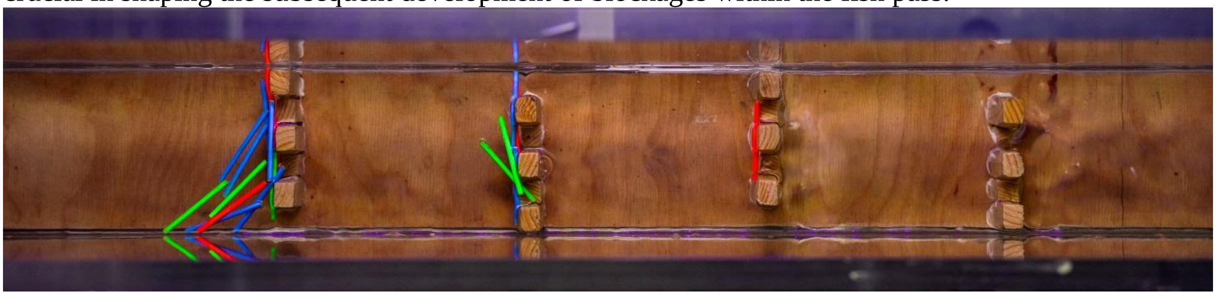

Fig. 14. Example of jamming. Accumulation of large wood (LW) at the first cross-wall. Example from test K0LT03. Flow direction from left to right

These findings reinforce the idea that local structural and flow conditions strongly influence debris retention, and that self-reinforcing jamming mechanisms may play a critical role in shaping the spatial pattern of accumulation inside fish passes.

To assess the overall efficiency of the fish pass structure in trapping debris, the EA values were averaged across all log size classes and measurement cross-sections. This aggregate indicator, referred to as EA_total, provides a global perspective on the impact of baffle shape on wood retention under uniform flow conditions.

Although the rectangular baffle configuration (K0) showed a higher average EA_total (0.24) compared to the rounded configuration (K1: 0.16), the difference was not statistically significant (p = 0.151, Wilcoxon test). The high variability in the data and the non-normal distribution of EA values (Shapiro-Wilk test) may have contributed to this outcome. Nonetheless, the observed ΔEA = 0.08 still points toward structural shape as a potentially important design parameter.

Although the rectangular baffles showed higher mean total accumulation, statistical analysis did not confirm a significant difference between the two shapes. Nonetheless, the observed tendency toward greater accumulation in the K0 configuration (EA = 0.24 vs. 0.16 for K1) may reflect underlying differences in how flow interacts with baffle geometry and wood elements. These patterns, while not statistically robust on a total scale, may still inform localized processes of retention observed elsewhere in the structure. However, this results must be interpreted with caution. Although comparing the total effective accumulation (EA_total) between the two baffle configurations provides a general overview of structural efficiency, it is important to acknowledge the substantial analytical limitations of this approach. EA_total is an aggregated metric that conceals key sources of variability—specifically, cross-wall section and log length. Previous analyses demonstrated that both of these factors significantly influence the probability of wood accumulation. Therefore, by examining only the average EA value, we disregard the internal structure of the data and potential interactions between variables. This simplification reduces the statistical power of the test and increases the risk of a Type II error (failing to reject a false null hypothesis). In other words, the lack of statistical significance in the EA_total analysis may result not from the absence of a real effect, but from an oversimplified model that fails to account for essential components of variability. Consequently, any generalizations based on this analysis should be made with particular caution.

The obtained results partially align with previous studies on wood accumulation around hydraulic obstacles; however, some discrepancies arise due to differences in flow conditions and structural geometry. Existing literature [48,82] emphasizes that rounded bridge piers exhibit a lower probability of wood accumulation due to their streamlined shape and reduced stagnation zones. In the case of fish passes, the results suggest a similar tendency—rounded structures (K1) facilitate lower wood retention. However, unlike bridge piers, wood in fish passes is confined within a narrow flow corridor, which may partially diminish the benefits of streamlined shapes.

One of the key factors determining wood accumulation is the Froude number (*Fr*), which affects log trajectories and their interactions with hydraulic obstacles. Researchers [52] have indicated that under subcritical flow conditions ($Fr < 1$), an increase in *Fr* generally leads to lower wood retention efficiency, particularly for isolated cylindrical obstacles, which is consistent with the results for K1 in this study.

Conversely, other studies [49] reported an opposite relationship—higher *Fr* values increased the probability of wood blockage on bridge piers. For $Fr = 0.5$, greater accumulation efficiency was observed compared to $Fr = 0.3$. The authors attributed this to variations in velocity distribution: at $Fr = 0.3$, velocity is more uniform, promoting unobstructed wood transport, whereas at $Fr = 0.5$, maximum velocity occurs along the channel axis, increasing the probability of log interaction with central obstacles. Under these conditions, logs are more prone to becoming trapped due to localized hydrodynamic effects, such as stagnation zones and secondary vortices.

In this study, the fish pass operated under constant flow conditions, meaning that baffles geometry, rather than dynamic changes in Fr, was the primary factor influencing wood accumulation. When the Froude number remains stable, the structural configuration becomes the dominant mechanism shaping accumulation processes.

The total EA analysis provides a global overview of wood accumulation, integrating effects across all log sizes and cross-wall locations. While the observed difference in total EA between K0 and K1 ($\Delta EA = 0.08$) suggests a potential influence of baffle geometry, this trend was not statistically confirmed and should be interpreted with caution.

These findings confirm earlier research indicating that baffles with rectangular cross-sections and flat surfaces (e.g., K0) promote wood retention by generating more pronounced flow disturbances around obstacles, increasing the probability of blockage [49]. At the same time, unlike bridge pier studies, the fish pass results suggest that baffle shape is the primary factor differentiating wood retention efficiency, as flow conditions were kept constant throughout the experiment.

Wood transport in river channels is a highly dynamic and complex process influenced by a range of hydraulic, structural, and morphodynamic factors. The literature emphasizes that wood blockage mechanisms depend heavily on how logs interact with hydraulic obstacles, as highlighted by [83]. Logs may (1) bypass an obstacle without contact, (2) make contact and continue downstream, (3) rebound off the obstacle and drift away, or (4) become effectively trapped on the obstacle. The complexity of wood transport processes in river systems results from the interplay between changing flow conditions and hydraulic structures. Local flow disturbances, secondary vortices, and rotational forces acting on individual logs can significantly alter their interaction with obstacles, leading to ambiguous outcomes.

Future research should account for both dynamic flow variations and a broader range of obstacle geometries to better understand the mechanisms responsible for wood transport and accumulation in different hydraulic systems.

Altogether, these findings reinforce the need for integrated design approaches that account for both geometric features and flow dynamics, particularly when fish pass structures are exposed to significant woody debris transport. The present study was limited to a single hydraulic scenario, corresponding to the nominal flow conditions observed at the reference fish pass ($Q = 3.85\ m^3/s$). This choice was made to ensure high repeatability of tests and focus on structural influence under stable conditions. Future work should include a broader range of discharges to examine flow-dependent accumulation behavior.

Finally, the interpretation of the presented results must take into account the potential influence of scale-related and methodological limitations inherent to laboratory modeling. Scaling in hydraulic models is a critical aspect of laboratory experiments, particularly when investigating sediment transport and hydrodynamic interactions with hydraulic structures. In this study, a 1:50 scale was applied, resulting in a significant reduction in dimensions compared to the full-scale fish pass. While this approach allows for precise control over experimental conditions, its potential limitations must be acknowledged, especially concerning surface tension effects and the physical properties of the model logs.

One notable limitation of laboratory scale models is the greater stability of model wood compared to natural river conditions. In the field, particularly during floods, logs may break apart under increased hydrodynamic forces, leading to dynamic changes in wood accumulation. Smaller fragments resulting from such breakage often continue downstream, reducing the probability of prolonged blockage. This fragmentation process was not observed in the laboratory experiments, likely because the model logs were more stable and not subjected to forces causing disintegration [84]. In full-scale conditions, fragmentation mechanisms may affect both blockage variability and wood retention time in hydraulic systems.

Another factor influencing wood transport scaling is the capacity of logs to absorb water. Research [85] has shown that wood mass can double after 24 hours of submersion, substantially altering buoyancy and transport behavior. In natural conditions, wood moisture varies, and prolonged water exposure can lead to partial submergence and changes in movement trajectories.

To prevent the effect of varying water absorption on experimental results, the logs were pre-soaked for several minutes before each test. This procedure aimed to ensure uniform moisture conditions for all wooden elements, in accordance with [85].

One observed scale effect was the influence of adhesion forces on wood, particularly in wood-to-wall interactions. During the experiments, cases were noted where individual logs “stuck” to the walls of the flume made of plexiglass. This was likely due to local surface tension forces and differences in material roughness. Such occurrences were treated as outliers and excluded from the EA analysis to prevent result distortion.

Although these cases were omitted from the final calculations, their occurrence highlights the need for caution when interpreting laboratory-scale results. Adhesion effects are negligible at full scale, where inertial and hydrodynamic forces dominate; however, in experimental conditions, they can influence wood transport and retention in the fish pass.

Therefore, additional tests at a larger scale are recommended to assess the impact of adhesion and potential differences in wood accumulation mechanisms under real hydraulic conditions.

Modelling wood transport and accumulation processes in hydraulic systems requires certain simplifications to standardize experimental conditions and facilitate result analysis. In this study, one key simplification was the use of smooth, cylindrical wooden dowels without branches or roots, which can significantly affect accumulation dynamics in natural rivers. This approach has also been applied in other studies on woody debris transport [4,50,86–90].

In natural rivers, wood often features branches, roots, and irregular shapes, which can significantly influence transport and blockage mechanisms. In reality, larger and more branched elements exhibit a greater surface area exposed to water flow, increasing the probability of obstruction at obstacles, as demonstrated in [20]. The probability of wood blockage increases with its size and decreases with the available freeboard, particularly in the context of bridge decks. Logs that include root systems display a substantially higher blockage probability than smooth, cylindrical ones because their irregular geometry favors snagging on structural components. Moreover, under higher Froude number conditions, the intensified flow forces can sometimes release already trapped wood, indicating that simplified log geometries used in laboratory tests may not fully replicate actual wood transport behavior in riverine environments.

Additionally, the natural process of wood jam formation is more complex and involves the deposition of smaller wood fragments in gaps and between larger logs, resulting in the formation of stable structures. A key role is played by the so-called "key member"—the initial large element that becomes lodged at the obstacle and initiates accumulation. Subsequently, smaller logs ("racked members") accumulate around it, while finer debris and organic materials fill the spaces between larger elements ("loose members"), stabilizing the structure [91–93].

In natural conditions, long-term biological processes can further enhance the stability and volume of accumulated wood. Trapped logs, particularly those from species capable of vegetative regrowth, can develop roots, branches, and leaves, leading to additional mass and an increased surface area interacting with flow. An example is willow wood (*Salix* sp.), which, when trapped in the fish pass at the Opatowice Weir, developed new shoots and leaves, creating a living structure that reinforced the blockage (Fig. a). Additionally, other plant species often colonize retained wood, using it as a habitat (Fig. b) [21,84,94,95]. In real conditions, anthropogenic debris such as plastic waste, films, and other synthetic materials frequently accumulates on wood jams, further stabilizing the blockage and increasing its volume [16].

Fig. 15. Examples of vegetation on retained wood in the fish pass at the Opatowice Weir (2022, Wrocław, Poland): a) Accumulated wood fragment (*Salix* sp.) sprouting new shoots; b) Wood fragment with developed herbaceous vegetation (*Poaceae*) colonizing the debris surface

In this study, the effects associated with the presence of branches, roots, vegetation, or plant colonization were not replicated, which may have resulted in a lower probability of wood blockage in the fish pass compared to real-world conditions. This is consistent with the findings of [20], who indicated that simplifying wood geometry can lead to an underestimation of the actual blockage risk in river systems. Nevertheless, in laboratory research, simplified geometry allows for the standardization of experimental conditions, which is crucial for ensuring comparability of results across different studies

[87]. However, future studies should consider incorporating tests with more complex wood shapes and observe the influence of vegetation and plant growth processes on the long-term stability of blockages.

These considerations underscore the importance of interpreting laboratory results within the appropriate experimental context and scaling assumptions, while also highlighting the potential benefits of extending future studies to more complex and realistic configurations.

In future stages of this research, numerical modeling is planned to complement the laboratory findings. CFD simulations could provide further insight into local flow structures around baffles and allow for parametric analyses under a wider range of hydraulic conditions. This approach would support a more comprehensive understanding of debris accumulation mechanisms in fish passes, particularly when extending to more complex geometries and variable flow regimes.

Although not part of the current study, complementary research has been carried out using the Iber-Wood module within the Iber 2D numerical modeling platform. While the results of this modeling are not included in the present article and remain unpublished, they offer promising directions for further investigation into wood accumulation processes.

Preliminary simulations conducted as part of this separate research effort highlighted several key differences between numerical and physical modeling approaches. For example, one of the most evident advantages of numerical simulation lies in the ability to precisely control the placement and orientation of logs. In laboratory conditions, even with standardized procedures, slight deviations in the insertion angle and entry position are unavoidable, which can affect the outcome. In contrast, the numerical model allows for perfect replication or controlled variability in these parameters, enabling isolation of specific influences such as angular dispersion.

Another important factor is flow control. In the laboratory flume, maintaining perfectly steady discharge—especially at low flow rates—is technically challenging due to system limitations and minor fluctuations. While these variations were minimized and likely insignificant in this study, the numerical model allows for truly constant boundary conditions. However, such idealization may not fully reflect natural variability observed in river systems.

At the same time, the Iber-Wood model introduces simplifications that limit its realism. Log–structure interactions are modeled as elastic collisions, without accounting for surface friction or deformation effects. Once a log touches a baffle, its new trajectory is calculated based on the angle of impact, which may lead to sliding or bouncing, but not actual retention [48].

Additional limitations include the lack of a skin friction drag coefficient and no adjustment of drag based on log orientation. In reality, surface texture and material friction between logs and structural components may significantly influence retention outcomes—particularly for rough or saturated wood. These aspects are not yet incorporated into Iber-Wood, which assumes smooth, frictionless dowels, and may thus underestimate blockage potential. Similar concerns have been raised in empirical studies such as [96], where natural logs showed higher drag forces due to bark and irregular geometry.

While these preliminary insights are not part of the present publication, they underscore the potential of combining laboratory and numerical methods. Future work may benefit from more advanced modeling features that better reflect the complex nature of wood accumulation, such as layered debris interactions, surface friction, and probabilistic log trajectories.

5. CONCLUSIONS

This study demonstrated that baffle geometry and log size significantly affect wood accumulation within vertical slot fish passes. Key findings are as follows:

- Baffle shape matters: Rounded baffles (K1) facilitated smoother debris passage and reduced accumulation, particularly in downstream sections. Rectangular baffles (K0) were associated with higher retention and localized blockages.
- Log size is a dominant factor: Longer logs were significantly more prone to retention, often triggering accumulation via bridging or wedging. Statistical analyses confirmed the size-dependent nature of accumulation patterns.
- Blockage formation followed jamming dynamics: Accumulation was amplified by previously retained logs, illustrating self-reinforcing "snowball" effects, especially for large elements.
- Design implications: Using rounded baffles can lower the risk of internal clogging and improve fish pass functionality, especially under conditions prone to woody debris input.
- Experimental limitations: Laboratory-scale simplifications—including cylindrical log geometry and constant flow—likely influenced accumulation behavior. Realistic features such as roots, branches, or variable buoyancy should be included in future research.
- Need for further investigation: Additional hydraulic scenarios and 2D/3D numerical modeling should be explored to improve generalizability and guide debris-resilient fish pass design.

ADDITIONAL INFORMATION

All statistical analyses and visualizations presented in this paper are fully reproducible. Supplementary materials [97] containing the complete dataset, code, and results are available at: https://doi.org/10.5281/zenodo.15629647

Table A. Conventional notation of statistical significance levels based on *p*-values

Symbol	***p***-value range	Statistical significance	Interpretation
***	$p < 0.001$	Highly significant	Strong evidence against the null hypothesis
**	$0.001 \leq p < 0.01$	Very significant	Clear evidence of an effect
*	$0.01 \leq p < 0.05$	Significant	Standard threshold for significance
. (dot)	$0.05 \leq p < 0.1$	Marginally significant (trend)	Weak or suggestive evidence
(blank) or — (em dash)	$p \geq 0.1$	Not significant	No statistical evidence

This notation follows conventional statistical reporting practices, where asterisks and symbols indicate significance thresholds based on *p*-values [98,99].

All figures and photographs are the author's own work (Jan Błotnicki), unless stated otherwise.

Special thanks are due to Professor Robert Głowski (orcid.org/0000-0002-2226-2306) for many years of cooperation, his supervisory guidance, and insightful comments—without which the preparation of this experiment would have taken considerably longer.
I would like to express my sincere gratitude to Dr. Maciej Gruszczyński (orcid.org/0000-0003-3663-2723) for his long-standing collaboration and invaluable support in all matters related to fishway hydraulics, as well as for his assistance in preparing the laboratory channel.

I am also deeply grateful to Dr. Paweł Jarzembowski (orcid.org/0000-0002-7869-7763), whose contribution significantly shaped the structure of the manuscript. His attention to scientific rigor and his recommendations regarding appropriate statistical tools were especially valuable.
The author extends gratitude to the head of the hydraulic laboratory, Dr. Michał Śpitalniak (orcid.org/0000-0002-9801-9388), for providing access to all available instruments and materials necessary for conducting the research.
Special thanks to Mr. Jan Janusz for his support, expertise, and manual work, which contributed to the preparation of the fish pass model.
Finally, I extend my heartfelt thanks to the anonymous reviewers who devoted substantial time and effort to carefully evaluate this work. Their thorough feedback, thoughtful suggestions, and recommendations for further analyses greatly contributed to improving the quality of this manuscript.

The APC/BPC is financed/co-financed by Wroclaw University of Environmental and Life Sciences.
The article is a part of a doctoral dissertation titled 'Modeling Woody Debris Flow in Fishways with Rounded Piers', prepared during doctoral studies at the Wrocław University of Environmental and Life Sciences.

REFERENCES

1. Rybníček, M, Kolář, T and Koňasová, E 2014. Dendrochronological dating of large woody debris on the example of Morávka River and Černá Opava River. *Acta Universitatis Agriculturae et Silviculturae Mendelianae Brunensis* **58**, 193–202.
2. Moulin, B and Piegay, H 2004. Characteristics and temporal variability of large woody debris trapped in a reservoir on the River Rhone (Rhone): implications for river basin management. *River Research and Applications* **20**, 79–97.
3. Ruiz-Villanueva, V, Díez-Herrero, A, Bodoque, JM and Bladé, E 2014. Large wood in rivers and its influence on flood hazard. Cuadernos de Investigación Geográfica, 40, 229–246.
4. Bocchiola, D, Rulli, MC and Rosso, R 2008. A flume experiment on the formation of wood jams in rivers. *Water Resources Research* **44**, 1–17.
5. Vaughn, T and Crookston, B M 2022. Influence of submerged woody debris at labyrinth weirs in river applications. *River Research and Applications* **38**, 235–244.
6. Allen, D, Arthur, S, Haynes, H, Wallis, S G and Wallerstein, N 2014. Influences and drivers of woody debris movement in urban watercourses. *Science China Technological Sciences* **57**, 1512–1521.
7. Mazur, R, Kałuża, T, Chmist, J, Walczak, N, Laks, I and Strzeliński, P 2016. Influence of deposition of fine plant debris in river floodplain shrubs on flood flow conditions – The Warta River case study. Physics and Chemistry of the Earth, Parts A/B/C, 94, 106–113.
8. Dudgeon, D, Arthington, AH, Gessner, MO, Kawabata, Z, Knowler, DJ, Lévêque, C, Naiman, RJ, Prieur-Richard, A, Soto, D, Stiassny, M L J and Sullivan, C A 2006. Freshwater biodiversity: importance, threats, status and conservation challenges. *Biological Reviews* **81**, 163–182.
9. Chan, JCF, Lam, BYK, Dudgeon, D and Liew, JH 2025. Global consequences of dam-induced river fragmentation on diadromous migrants: a systematic review and meta-analysis. Biological Reviews, 1–18.
10. Silva, AT, Lucas, MC, Castro-Santos, T, Katopodis, C, Baumgartner, LJ, Thiem, JD, Aarestrup, K, Pompeu, PS, O'Brien, G C, Braun, D C, Burnett, N J, Zhu, D Z, Fjeldstad, H, Forseth, T, Rajaratnam, N, Williams, J G and Cooke, S J 2018. The future of fish passage science, engineering, and practice. *Fish and Fisheries*, **19**, 340–362.

11. Błotnicki, J, Głowski, R and Gruszczyński, M 2022. Ograniczenie drożności przepławki dla ryb w wyniku stagnacji rumowiska pływającego [Reduced Passability of a Fishway Due to the Stagnation of Floating Debris]. XXXIX Ogólnopolska Szkoła Hydrauliki "Ochrona przed powodzią i suszą - duża i mała retencja," Kraków 1–1.
12. Błotnicki, J 2020. Hydraulic flow parameters in a fishway contaminated with remaining wooden debris. In: Kostecki, J and Jakubaszek, A (ed) 4th Conference "Environmental Engineering and Design," Zielona Góra: University of Zielona Góra 20–20.
13. Mumot, J and Tymiński, T 2016. Hydraulic research of sediment transport in the vertical slot fish passes. *Journal of Ecological Engineering* **17**, 143–148.
14. Diehl, TH 1997. Potential Drift Accumulation at Bridges. US Department of Transportation, Federal Highway Administration, Research and Development, Turner-Fairbank Highway Research Center, 1–45.
15. Bradley, JB, Richards, DL and Bahner, CD 2005. Debris control structures: Evaluation and countermeasures. Report No. FHWA-IF-04-016, Hydraulic Engineering Circular Washington, DC.
16. Błotnicki, J, Buta, B, Głowski, R and Jarzembowski, P 2025. Drifting Impact: A Comprehensive Review of Floating Debris. *Preprints,* 2025011125.
17. Shumilova, O, Tockner, K, Gurnell, AM, Langhans, SD, Righetti, M, Lucía, A and Zarfl, C 2019. Floating matter: a neglected component of the ecological integrity of rivers. *Aquatic Sciences* **81**, 25.
18. Pollard, D, DeConto, RM and Alley, RB 2018. A continuum model (PSUMEL1) of ice mélange and its role during retreat of the Antarctic Ice Sheet. *Geoscientific Model Development* **11**, 5149–5172.
19. Słowik-Opoka, E, Michno, A and Jarosz, A 2024. Effects of woody debris on alluvial sediment differentiation and particulate organic matter accumulation in a mountainous forest stream in the Polish Carpathians. *Frontiers in Forests and Global Change* **7**, 1–16.
20. Schmocker, L and Hager, W H 2011. Probability of Drift Blockage at Bridge Decks. *Journal of Hydraulic Engineering* **137**, 470–479.
21. Sass, G G 2009. Coarse Woody Debris in Lakes and Streams. *Encyclopedia of Inland Waters*, 60–69.
22. Montgomery, DR and Abbe, TB 1996. Large woody debris jams, channel hydraulics and habitat formation in large rivers. *Regul. Rivers, Res. Mgmt* **12**, 201–221.
23. Bocchiola, D, Rulli, MC and Rosso, R 2006. Flume experiments on wood entrainment in rivers. *Advances in Water Resources* 29, 1182–1195.
24. Harmon, ME, Franklin, JF, Swanson, FJ, Lattin, JD, Cline, SP, Harmon, ME, Franklin, JF and Swanson, FJ 1986. *Ecology of Coarse Woody Debris in Temperate Ecosystems Ecology of Coarse Woody Debris in Temperate Ecosystems* vol 15.
25. Gurnell, AM, Gregory, KJ and Petts, GE 1995. The role of coarse woody debris in forest aquatic habitats: Implications for management. *Aquatic Conservation: Marine and Freshwater Ecosystems* **5**, 143–166.
26. Maricar, MF, Maricar, F, Lopa, RT and Hashimoto, H 2020. Flume experiments on log accumulation at the bridge with pier and without pier. *IOP Conference Series: Earth and Environmental Science* **419**, 012124.
27. Rasche, D, Reinhardt-Imjela, C, Schulte, A and Wenzel, R 2019. Hydrodynamic simulation of the effects of stable in-channel large wood on the flood hydrographs of a low mountain range creek, Ore Mountains, Germany. *Hydrology and Earth System Sciences* **23**, 4349–4365.
28. Maricar, MF and Maricar, F 2020. Flume experiments on woody debris accumulation at the bridge pier during flood. *IOP Conference Series: Earth and Environmental Science* **575**, 012188.

29. Lagasse, PF, Clopper, PE, Zevenbergen, LW, Spitz, WJ and Girard, LG 2010. *Effects of Debris on Bridge Pier Scour* Washington, D.C.: Transportation Research Board.
30. Ruiz-Villanueva, V, Gamberini, C, Bladé, E, Stoffel, M and Bertoldi, W 2020. Numerical Modeling of Instream Wood Transport, Deposition, and Accumulation in Braided Morphologies Under Unsteady Conditions: Sensitivity and High-Resolution Quantitative Model Validation. *Water Resources Research* **56**, e2019WR026221.
31. Ruiz-Villanueva, V, Wyżga, B, Hajdukiewicz, H and Stoffel, M 2016. Exploring large wood retention and deposition in contrasting river morphologies linking numerical modelling and field observations. *Earth Surface Processes and Landforms* **41**, 446–459.
32. van Emmerik, T and Schwarz, A 2020. Plastic debris in rivers. *WIREs Water* **7**, 1–24.
33. Liro, M, Mikuś, P and Wyżga, B 2022. First insight into the macroplastic storage in a mountain river: The role of in-river vegetation cover, wood jams and channel morphology. *Science of The Total Environment* **838**, 156354.
34. Liro, M, Zielonka, A, Hajdukiewicz, H, Mikuś, P, Haska, W, Kieniewicz, M, Gorczyca, E and Krzemień, K 2023. Litter Selfie: A Citizen Science Guide for Photorecording Macroplastic Deposition along Mountain Rivers Using a Smartphone. *Water* **15**, 3116.
35. Błotnicki, J 2020. Problem of floating debris. In: Kostecki, J and Jakubaszek, A (ed) *4 th CONFERENCE "ENVIRONMENTAL ENGINEERING AND DESIGN,"* Zielona Góra: University of Zielona Góra 21.
36. Ruiz-Villanueva, V, Wyżga, B, Zawiejska, J, Hajdukiewicz, M and Stoffel, M 2016. Factors controlling large-wood transport in a mountain river. *Geomorphology* **272**, 21–31.
37. Swanson, FJ, Gregory, SV, Iroumé, A, Ruiz-Villanueva, V and Wohl, E 2020. Reflections on the history of research on large wood in rivers. *Earth Surface Processes and Landforms* **66**, 55–66.
38. Ruiz-Villanueva, V, Wyżga, B, Mikuś, P, Hajdukiewicz, H and Stoffel, M 2016. The role of flood hydrograph in the remobilization of large wood in a wide mountain river. *Journal of Hydrology* **541**, 330–343.
39. Poledniková, Z and Galia, T 2020. Large wood and the concept of ecosystem services. *River Flow 2020*, CRC Press 1694–1700.
40. Grabowski, RC, Gurnell, AM, Burgess-Gamble, L, England, J, Holland, D, Klaar, MJ, Morrissey, I, Uttley, C and Wharton, G 2019. The current state of the use of large wood in river restoration and management. *Water and Environment Journal* **33**, 366–377.
41. Błotnicki, J, Gruszczyński, MMF, Głowski, R and Mokwa, M 2024. Enhancing migratory potential in fish passes: The role of pier shape in minimizing debris accumulation. *Journal of Environmental Management* **359**, 121053.
42. Xiang, F, Kavvas, LM, Chen, Z, Bandeh, H, Ohara, N, Kim, S, Jang, S-H and Churchwell, R 2009. Experimental study of debris capture efficiency of trash racks. *Journal of Hydro-environment Research* **3**, 138–147.
43. Wiering, V and Heneka, P 2013. Experimental Study of Driftwood Deflectors at Fishway Intakes. *Proceedings of the 40th IAHR World Congress*, Vienna, Austria 2023–2029.
44. Larinier, M 2002. Fishways: biological basis, design criteria and monitoring. *Bulletin Français de la Pêche et de la Pisciculture*, Boves, France : Conseil supérieur de la pêche ; [Rome] : Food and Agriculture Organization of the United Nations ; [Antony, France] : Cemagref Editions 39–53.
45. Larinier, M 2002. Fishways - General considerations. *Bulletin Français de la Pêche et de la Pisciculture* **364**, 21–27.
46. Błotnicki, J, Gruszczyński, M, Jarzembowski, P and Popczyk, M 2023. Application of close-range remote sensing for automatic identification of ice jams in rivers in the area of the inlet to the fishway. *Zeszyty Naukowe / Akademia Morska w Szczecinie* **75**, 97–106.

47. Błotnicki, J, Jarzembowski, P, Gruszczyński, MF and Popczyk, MK 2023. The Use of UAV for Measuring the Morphology of Ice Cover on the Surface of a River: A Case Study of the Low Head Dam and Fishway Inlet Area in the Odra River. *Water* **15**, 3972.
48. De Cicco, P N 2017. Experimental and numerical investigations on wood accumulation at bridge piers with different shapes [Doctoral dissertation, University of Florence] University of Florence.
49. De Cicco, PN, Paris, E, Solari, L and Ruiz-Villanueva, V 2020. Bridge pier shape influence on wood accumulation: Outcomes from flume experiments and numerical modelling. *Journal of Flood Risk Management* **13**, 1–16.
50. Braudrick, CA, Grant, GE, Ishikawa, Y and Ikeda, H 1997. Dynamics of Wood Transport in Streams: A Flume Experiment. *Earth Surface Processes and Landforms* **22**, 669–683.
51. Gruszczyński, M and Błotnicki, J 2020. Badanie ruchu rumowiska polifrakcyjnego w szczelinowej przepławce dla ryb. In: Kałuża, T, Radecki-Pawlik, A, Wiatkowski, M and Hammerling, M (ed) *Modelowanie procesów hydrologicznych Zagadnienia modelowania w sektorze gospodarki wodnej*, Poznań: Bogucki Wydawnictwo Naukowe 87–104.
52. Chowdhury, P, Fredericks, I, Alvarez, JC, Clark, M, Jayaratne, R, Wijetunge, JJ, Raby, A and Taylor, P 2024. Mixed debris interaction with obstacle array under extreme flood conditions. *Journal of Flood Risk Management* **17**, 1–14.
53. R Core Team 2025. R: A Language and Environment for Statistical Computing.
54. Team, P 2025. RStudio: Integrated Development Environment for R.
55. Wickham, H, François, R, Henry, L, Müller, K and Vaughan, D 2023. dplyr: A Grammar of Data Manipulation.
56. Wickham, H, Vaughan, D and Girlich, M 2024. tidyr: Tidy Messy Data.
57. Wickham, H 2016. *ggplot2: Elegant Graphics for Data Analysis* Springer-Verlag New York.
58. Ogle, DH, Doll, JC, Wheeler, AP and Dinno, A 2025. FSA: Simple Fisheries Stock Assessment Methods.
59. Kay, M, Elkin, LA, Higgins, JJ and Wobbrock, JO 2025. {ARTool}: Aligned Rank Transform for Nonparametric Factorial ANOVAs.
60. Wobbrock, JO, Findlater, L, Gergle, D and Higgins, JJ 2011. The aligned rank transform for nonparametric factorial analyses using only anova procedures. *Proceedings of the SIGCHI Conference on Human Factors in Computing Systems*, New York, NY, USA: ACM 143–146.
61. Elkin, LA, Kay, M, Higgins, JJ and Wobbrock, JO 2021. An Aligned Rank Transform Procedure for Multifactor Contrast Tests. *Proceedings of the ACM Symposium on User Interface Software and Technology (UIST '21)*, New York: ACM Press 754–768.
62. Pearce, SC 1992. Introduction to Fisher (1925) Statistical Methods for Research Workers. 59–65.
63. Shapiro, SS and Wilk, MB 1965. An Analysis of Variance Test for Normality (Complete Samples). *Biometrika* **52**, 591.
64. Kruskal, WH and Wallis, WA 1952. Use of Ranks in One-Criterion Variance Analysis. *Journal of the American Statistical Association* **47**, 583–621.
65. Dunn, O J 1964. Multiple Comparisons Using Rank Sums. *Technometrics* **6**, 241–252.
66. Wilcoxon, F 1945. Individual Comparisons by Ranking Methods. *Biometrics Bulletin* **1**, 80.
67. Tukey, JW 1949. Comparing Individual Means in the Analysis of Variance. *Biometrics* **5**, 99.
68. Blanca, M, Alarcón, R, Arnau, J, Bono, R and Bendayan, R 2017. Non-normal data: Is ANOVA still a valid option?. *Psicothema* **4**, 552–557.
69. Lix, LM, Keselman, JC and Keselman, HJ 1996. Consequences of Assumption Violations Revisited: A Quantitative Review of Alternatives to the One-Way Analysis of Variance "F" Test. *Review of Educational Research* **66**, 579.

70. Corredor-Garcia, JL, Delalande, A, Stovin, V and Guymer, I 2020. On the Use of Surface PIV for the Characterization of Wake Area in Flows Through Emergent Vegetation. *GeoPlanet: Earth and Planetary Sciences*, 43 – 52.
71. Ruan, C, Sun, C-D, Bai, Y-L, Wang, Y-S, Ren, K-H and Feng, S 2006. Characteristics of the tracer particles used in water flow field for PIV system. *Shiyan Liuti Lixue/Journal of Experiments in Fluid Mechanics* **20**, 72 – 77.
72. Kundu, PK and Cohen, IM 2002. *Fluid Mechanics* San Diego: Academic Press.
73. Ruiz-Villanueva, V, Piégay, H, Gurnell, AA, Marston, RA and Stoffel, M 2016. Recent advances quantifying the large wood dynamics in river basins: New methods and remaining challenges. *Reviews of Geophysics* **54**, 611–652.
74. Wang, M, Wu, S, Chen, Y and Luan, W 2025. The snowball effect in electrochemical degradation and safety evolution of lithium-ion batteries during long-term cycling. *Applied Energy* **378**, 124909.
75. Dror, IE 2025. Biased and Biasing: The Hidden Bias Cascade and Bias Snowball Effects. *Behavioral Sciences* **15**, 490.
76. De Gregorio, P, Lawlor, A, Bradley, P and Dawson, KA 2005. Exact solution of a jamming transition: Closed equations for a bootstrap percolation problem. *Proceedings of the National Academy of Sciences* **102**, 5669–5673.
77. Sugiyama, Y, Fukui, M, Kikuchi, M, Hasebe, K, Nakayama, A, Nishinari, K, Tadaki, S and Yukawa, S 2008. Traffic jams without bottlenecks—experimental evidence for the physical mechanism of the formation of a jam. *New Journal of Physics* **10**, 033001.
78. Gallisdorfer, MS, Bennett, SJ, Ghaneeizad, SM, Atkinson, JF, Mohammad, S and Atkinson, JF 2016. Morphodynamic responses of physical-scale experimental river channels to engineered log jams for stream restoration design. *River Flow 2016*, Taylor & Francis Group, 6000 Broken Sound Parkway NW, Suite 300, Boca Raton, FL 33487-2742: CRC Press 2354–2358.
79. L'Hommedieu, W, Tullos, D and Jones, J 2020. Effects of an engineered log jam on spatial variability of the flow field across submergence depths. *River Research and Applications* **36**, 383–397.
80. Lai, YG, Smith, DL, Bandrowski, DJ, Liu, X and Wu, K 2017. Three Dimensional Computational Modeling of Flows through an Engineered Log Jam. *World Environmental and Water Resources Congress 2017*, Reston, VA: American Society of Civil Engineers 16–23.
81. Lai, YG 2024. On the Drag Force of Flows over Engineered Log Jams. *World Environmental and Water Resources Congress 2024*, Reston, VA: American Society of Civil Engineers 846–854.
82. De Cicco, P , Paris, E and Solari, L 2015. Flume experiments on bridge clogging by woody debris: the effect of shape of piers. *E-proceedings of the 36th IAHR World Congress 28 June – 3 July, 2015, The Hague, the Netherlands*, 1–5.
83. Adachi, S and Daido, A 1957. *Experimental study on washed timbers* Kyoto.
84. Braudrick, CA and Grant, GE 2001. Transport and deposition of large woody debris in streams: a flume experiment. *Geomorphology* **41**, 263–283.
85. Thevenet, A, Citterio, A and Piegay, H 1998. A new methodology for the assessment of large woody debris accumulations on highly modified rivers (example of two french piedmont rivers). *River Research and Applications* **14**, 467–483.
86. Allen, JB and Smith, DL 2012. Characterizing the Impact of Geometric Simplification on Large Woody Debris Using CFD. *International Journal of Hydraulic Engineering* **1**, 1–14.
87. Xu, Y and Liu, X 2016. 3D computational modeling of stream flow resistance due to large woody debris. *River Flow 2016*, Taylor & Francis Group, 6000 Broken Sound Parkway NW, Suite 300, Boca Raton, FL 33487-2742: CRC Press 2346–2353.

88. Ruiz-Villanueva, V, Bladé, E, Sánchez-Juny, M, Marti-Cardona, B, Díez-Herrero, A and Bodoque, J M 2014. Two-dimensional numerical modeling of wood transport. *Journal of Hydroinformatics* **16**, 1077–1096.
89. Buxton, TH 2010. Modeling entrainment of waterlogged large wood in stream channels. *Water Resources Research* **46**, 1–15.
90. Gschnitzer, T, Gems, B, Aufleger, M, Mazzorana, B and Comiti, F 2013. Physical Scale Model Test on Bridge Clogging. *Proceedings of the 35th IAHR World Congress. Beijing: Tsinghua University Press,* Beijing: Beijing: Tsinghua University Press, ISBN 978-7-89414-588-8.
91. Abbe, TB, Brooks, AP and Montgomery, DR 2003. Wood in River Rehabilitation and Management. *American Fisheries Society Symposium*, 1–25.
92. Curran, JC 2010. Mobility of large woody debris (LWD) jams in a low gradient channel. *Geomorphology* **116**, 320–329.
93. Wallerstein, NP and Thorne, CR 1997. Impacts of Woody Debris on Fluvial Processes and Channel Morphology in Stable and Unstable Streams.
94. Antón, A, Elosegi, A, García-Arberas, L, Díez, J and Rallo, A 2011. Restoration of dead wood in Basque stream channels: Effects on brown trout population. *Ecology of Freshwater Fish* **20**, 461–471.
95. Le Lay, YF, Piégay, H and Moulin, B 2013. Wood Entrance, Deposition, Transfer and Effects on Fluvial Forms and Processes: Problem Statements and Challenging Issues. vol 12 *Treatise on Geomorphology*, Elsevier Inc. 20–36.
96. Merten, E, Finlay, J, Johnson, L, Newman, R, Stefan, H and Vondracek, B 2010. Factors influencing wood mobilization in streams. *Water Resources Research* **46**, W10514.
97. Błotnicki, J 2025. Designing For Flow: How Baffle Geometry Shapes Wood Accumulation In Fishways (Supplementary Materials) (v1.1.0) [Data set].
98. Wasserstein, RL and Lazar, NA 2016. The ASA Statement on p -Values: Context, Process, and Purpose. *The American Statistician* **70**, 129–133.
99. Field, A 2013. Discovering Statistics Using IBM SPSS Statistics London: Sage Publications.
100. Piepho, H-P 2004. An Algorithm for a Letter-Based Representation of All-Pairwise Comparisons. *Journal of Computational and Graphical Statistics* **13**, 456–466.